

R&D Proposal for a Fast, Radiation-Hard Calorimeter Subsystem for the SSC

Contact Person: Daryl D. DiBitonto¹⁾

Co-Investigators:

Barbara Bishop²⁾, Jerome Busenitz¹⁾, Peter Fu²⁾, Tony Gabriel²⁾,
Kuok-Young Ling³⁾, Hain-Ching Liu³⁾, Dipayan Mazumdar¹⁾,
Mark Timko¹⁾, Larry Wurtz¹⁾, and Peter Van Peteghem³⁾

1) Department of Physics and Astronomy
The University of Alabama
Tuscaloosa, Alabama 35487-0324

2) Oak Ridge National Laboratory
Physics Division
Oak Ridge, Tennessee 37831-6369

3) Department of Electrical Engineering
Texas A&M University
College Station, Texas 77843-3128

Submitted by
Office for Sponsored Programs
The University of Alabama
Tuscaloosa, Alabama 35487-0324

September 1989

Summary

We propose an R&D program for a fast, radiation-hard calorimeter readout subsystem for the SSC. This work is a continuation and extension of research already supported by the generic detector R&D program to develop fast warm liquid calorimetry for the SSC. The primary research emphasis of this proposal is now to develop a complete fast electronic readout subsystem for this technology, using prototype warm liquid vessels presently under construction as a testing reference. A principal design feature of the proposed subsystem is a level sensitive readout whose sampling frequency is matched to the SSC beam crossing frequency. With this system slow and inexpensive warm liquid media such as TMP can then be used within the calorimeter, while at the same time allowing this detector to respond sufficiently fast for use as a triggering device.

We also propose a study of the optimal longitudinal segmentation within a warm liquid calorimeter. For particular physics applications where the local energy loss through the detector must be measured, the configuration and grouping of individual detector cells must then be optimized for energy resolution and acceptance on the basis of detector response. Design simulations based on the CALOR89 code developed at the Oak Ridge National Laboratory will be used in these studies. Test beam studies of the entire subsystem as proposed are planned for a warm liquid test facility presently being built at Fermilab.

Table of Contents

I. Proposed Subsystem R&D	2.
II. Conceptual Calorimeter Design	4.
III. Proposed Measurement Electronics	8.
IV. R&D Manpower Commitments and Milestones	23.
V. Budget Justification	27.
References	29.
Tables	31.
Budget Detail	33.
Appendices	36.
Curriculum Vitae	

I. Proposed Subsystem R&D

The choice of detector technology for hadron calorimetry at the SSC depends largely on the design considerations of detector medium speed, segmentation, and radiation hardness. As one of the candidate technologies emerging for possible application at the SSC, warm liquid hydrocarbon media appear to satisfy most detector requirements for radiation hardness^{1),2)} and segmentation (either as longitudinally segmented modular vessels, or as integrated "swimming pool" type detectors). With the proper choice of radiator to detector medium ratio, warm liquid calorimetry can be made compensating³⁾ whereby electromagnetic and hadronic measurements are both integrated into the same structure. Unfortunately the drift time of free electrons in these fluids is still too slow to compete with the fast 16 nsec crossing time expected at the SSC. Even in a high mobility fluid medium like TMS, the maximum drift time across a 1 mm gap is only 100 nsec at the present maximum operating field⁴⁾ of 10^4 V/cm. Alternative electrode designs have been studied to increase this internal electric field⁵⁾. However, the intrinsic low mobilities of fluids such as TMP and TMS still remain a fundamental limitation. Most accompanying readout electronics designed for this application⁶⁾ are usually too slow to compete with the SSC repetition rate, since they must integrate over many beam crossings to achieve the required sensitivity of roughly 1000 electrons.

Willis and Radeka⁷⁾ have pointed out that the current waveforms produced by the passage of ionizing radiation within a liquid ionization cell contains information on the total charge present at any given time. In an ideal detector with negligible source resistance and inductance and high liquid purity, this current profile is saw-toothed in nature, with the maximum signal current level occurring at the very beginning of the pulse. At the SSC where the total drift time may span many beam crossings, the superposition of consecutive interactions passing through the same cell can still provide information on the total amount of charge deposited in any given crossing by comparing the (current) levels present at the beginning of consecutive pulses of interest. This can be achieved with a level sensitive readout system whose sampling frequency is matched to the beam crossing frequency. These

levels can then be digitized and stored into a cycling memory and compared later via a fast, simple pattern recognition comparison to extract the individual charge information. We propose to develop such a readout subsystem for the SSC.

A direct advantage of this fast readout approach is that traditionally "slow" liquids such as TMP can now be used in these detectors, since the drift time provides a (decreasing) baseline onto which relative charge deposited from each beam crossing can be measured. Furthermore, TMP is presently one of the cheapest warm liquid hydrocarbons manufactured commercially, thus significantly reducing the potential cost of a large warm liquid calorimeter system based on what otherwise may be a more exotic technology such as TMS or possibly TMGe.

A readout scheme such as the one proposed is feasible only when the source capacitance is typically less than 100-200 pF⁸⁾. This limit is based on present day values of semiconductor device specifications for monolithic implementation of a charge preamplifier designed for this purpose. In addition to low source capacitance, the lead inductance and resistance must also be kept low to maintain an intrinsic detector response (RC and $1/\sqrt{LC}$ time constants) much faster than the beam crossing time of 16 nsec. To this end the charge preamplifier should ideally be located as close to the detector as possible. With this constraint on location, the corresponding electronic circuitry must be sufficiently radiation hardened to operate reliably.

We have recently developed a fast, 5 Mrad radiation-hard charge preamplifier for warm liquid calorimetry⁹⁾ based on an industrial BiFET process with less than 3.5 nV/ $\sqrt{\text{Hz}}$ noise and with a 37 nsec risetime (see Appendix I). A modified circuit of similar design¹⁰⁾ has recently been submitted for industrial implementation in a 1 Grad BiFET technology with a 10 nsec risetime, and we are presently designing a 5 nsec version in the same Grad technology. Prototype warm liquid cells with low source capacitance and high internal electric fields are also being developed^{5),10)} that are matched to the speed and sensitivity requirements of this preamplifier (see Appendix II). Together these cells and charge preamplifiers will serve to develop a fast prototype warm liquid calorimeter.

The final detector configuration will necessarily depend on a variety of physics inputs such as acceptance, energy resolution, and hermeticity suitable to the needs of a given physics program. In the case of muon identification, the total cross section for muon bremsstrahlung in an ordinary hadron calorimeter is not large, although this bremsstrahlung contributes to a tail of catastrophic loss to the muon energy loss distribution¹¹⁾. Proper modelling of these effects is therefore necessary to optimize the longitudinal segmentation required for a given degree of measured 4-momentum accuracy. As part of our research program we will investigate the simulated design response of such a longitudinally segmented calorimeter with the CALOR89 code developed at the Oak Ridge National Laboratory.

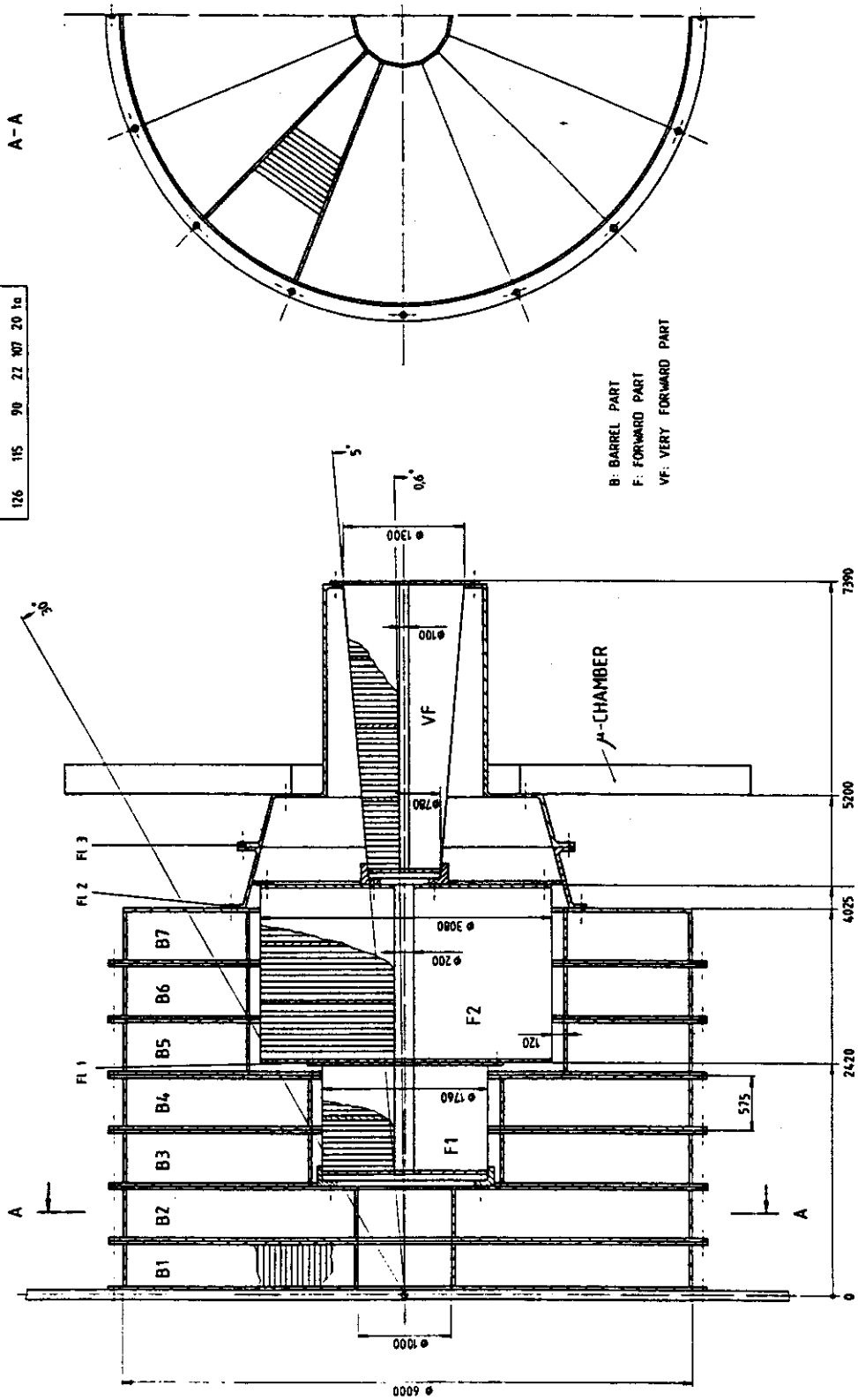
II. Conceptual Calorimeter Design

A preliminary design study of a hadron calorimeter for an SSC experiment has recently been proposed by Aachen¹²⁾ (Prof. Dr. Klaus Lübelmeyer and Dr. Ing. Klaus Genius). In this conceptual design, shown in Figure 1, the calorimetry has been configured with muon identification in mind. The hadron calorimeter in Figure 1 is roughly 10-12 absorption lengths thick and has been organized in projective towers with as of yet unspecified transverse segmentation. One half of the calorimeter consists of a barrel region (B1-B7), a forward region (F1, F2), and a very forward region (VF). In this particular configuration they have indicated longitudinal segmentation of the calorimeter away from the central collision point with alternating radiator and detector. This modular design allows greater independence in the choice of radiator material and detector medium, while allowing longitudinal sampling of the energy flow of particles passing through the calorimeter.

Each barrel part consists of 7 sections of rings or hexagonal rings with radial flanges at the barrel rings. They in turn contain detection chambers which lay parallel to the axial direction. The forward parts consist of two cylindrical parts each divided into two and three compartments, while the very forward conical part is divided into three compartments. Each part contains detection chambers which lay parallel to the radial direction.

MASSES

B1B2	63.84	85-87	F1	F2	VF
126	115	90	22	107	20 kg



B: BARREL PART
 F: FORWARD PART
 VF: VERY FORWARD PART

HADRON-CALORIMETER FOR A COLLIDER EXPERIMENT

I. PHYSIKALISCHES INSTITUT, RWTH AACHEN

INGENIEURBERATUNG MARCH
 DR.-ING. RUDOLF
 THIESSENSTR. 28, 5100 AACHEN (FR)

Project No.	126
Scale	1:1
Date	1978
Author	R. Thies
Checked	
Approved	

Figure 1. Conceptual Design for an SSC Hadron Calorimeter (from ref. 12).

The total weight of the calorimeter is roughly 1800 tons and the weight of the support structure is estimated at roughly 200 tons. In Table I the estimates for wall thicknesses and barrel ring flanges are given. The thickness of the flanges at the barrel rings is estimated to be $B = 30$ mm.

The assembly of the hadron calorimeter would be done by device on rails. First the barrel parts B1-B4 are fixed at their respective bearing plates. Then part F1 is transported by means of the flange F1 1 and rolled in on rails laying in barrel B3-B4 or laid directly on the wall of B4. Next the assembly of the barrel B5-B7 is completed in the same way as before. F2 is taken at flange F1 2 and can be rolled into B5-B6 on rails or be connected directly at B7. VF is then transported by means of flange F1 3 and fixed at the assembled structures.

We propose to develop fast readout electronics for a representative projective "tower" (pointing to the main interaction region) that would be found within one of these three detector regions. The corresponding longitudinal segmentation may indeed be different, depending on the specific physics requirements for energy detection in a given calorimeter region. Each detector cell will be read out with its own separate charge preamplifier and then summed together in larger groups, which can then be separately digitized and read out to a data buffer. Although the longitudinal segmentation may be high, the actual reduction in digitizing, buffering, and readout components per tower can be significant by grouping large numbers of cells into a single cluster. The exact calorimeter configuration will depend on the specific physics application and measurement requirements; our goal is to design such a detection and readout system with this flexibility in mind.

Prototype warm liquid cells designed for a small, compact calorimeter to instrument the forward collider region^{5),8)} are presently under construction at Coors Ceramics and at Hutchinson Technology, Inc. (see Figure 2). We propose to assemble a representative tower from these prototype cells and suitably chosen radiator material and develop the electronics readout system in an actual test beam environment. A description of these cells is given in Appendix II.

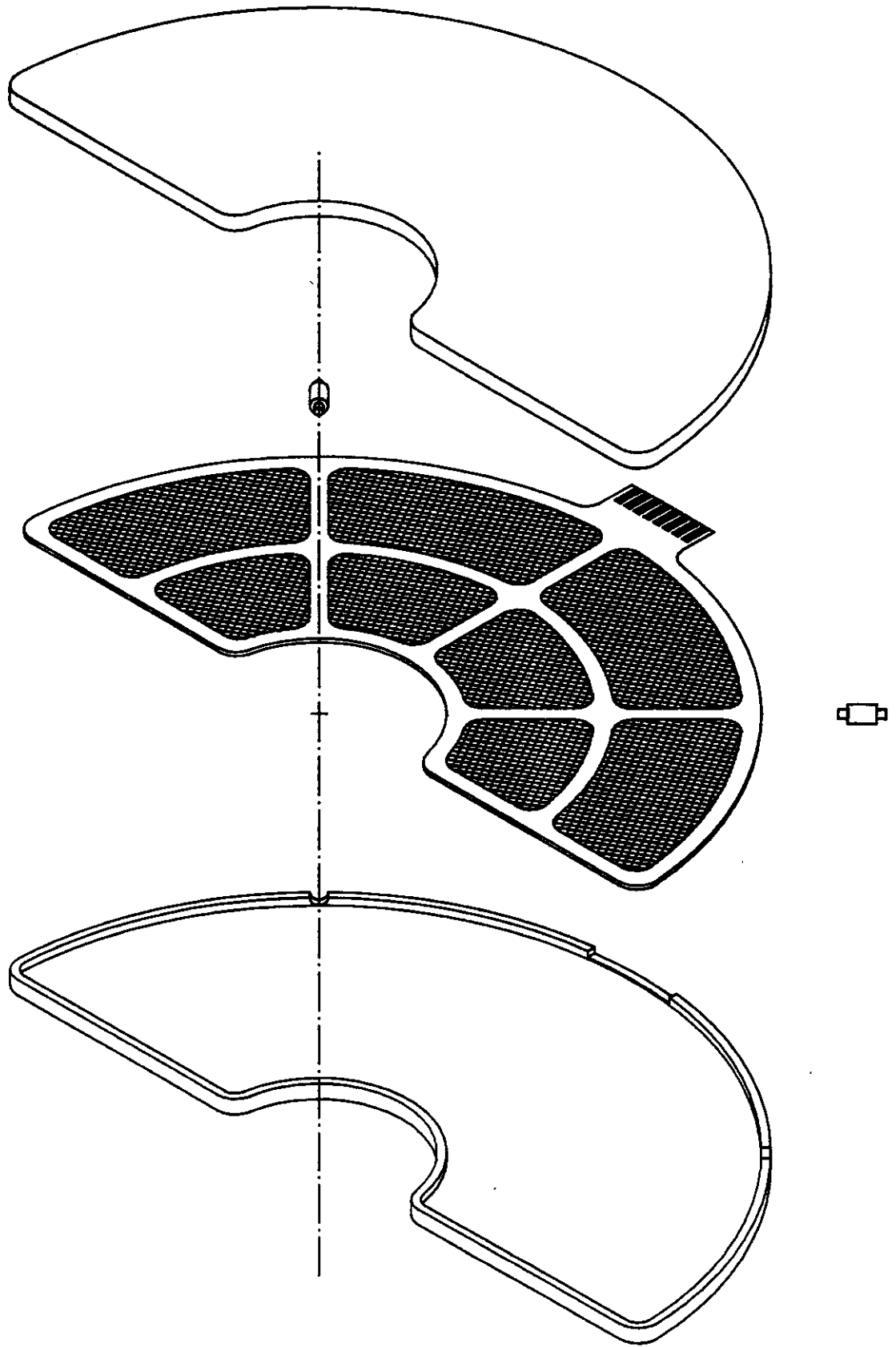


Figure 2. Prototype warm liquid cell.

III. Proposed Measurement Electronics

A schematic diagram of the proposed calorimetry measurement electronics is shown in Figure 3. A four chip set consisting of a front-end charge preamplifier, summer chip, digitizer, and buffer cell defines the calorimetry measurement within a projective tower. The preamplifier and summer chips are located immediately after the detector output, while the digitizer and buffer circuits are located on the outer periphery of the calorimeter. The preamplifier chip is designed to accommodate nine charge preamplifiers, eight of which are connected to a detector and an additional preamplifier on the same substrate from which baseline noise information will be collected. Each preamplifier is optimized for a particular detector capacitance. Several preamplifier designs are now under investigation with the most promising design being fabricated in a 1 Grad BiFET technology. The proposed summer chip is configured in the measurement system to reduce the number of analog-to-digital converters (ADC). Each summer is proposed to handle at least four preamplifiers and, accordingly, at least four detector channels within a tower with output connected to the input of a single ADC. The summer chip will also be fabricated in the same 1 Grad BiFET technology mentioned above. Both the preamplifier and summer chips are proposed for physical location as close to their respective detectors as possible. Shielded cables will connect the summer outputs with the following electronics which is proposed for placement on the surface of the calorimetry measurement system outside the region of intense radiation.

The digitizer and buffer cell (DBC) shown in Figure 3 contains a high-speed eight-bit ADC and enough buffer memory to handle one μsec of data per channel. A high speed eight-bit ADC based on a gray-code multiple folding circuit with conversion time comparable to flash-ADC techniques¹³⁾ at a fraction of the component count and chip layout area is presently being studied. The readout control chip has a second level buffer and readout control sequencer which will accommodate 15 μsec of data per channel. The data will be sent to a control room after a second-level trigger signal has been received. Both the DBC and readout control chips are under design in a high-radiation CMOS technology to increase packing density and reduce power dissipation^{14),15)}.

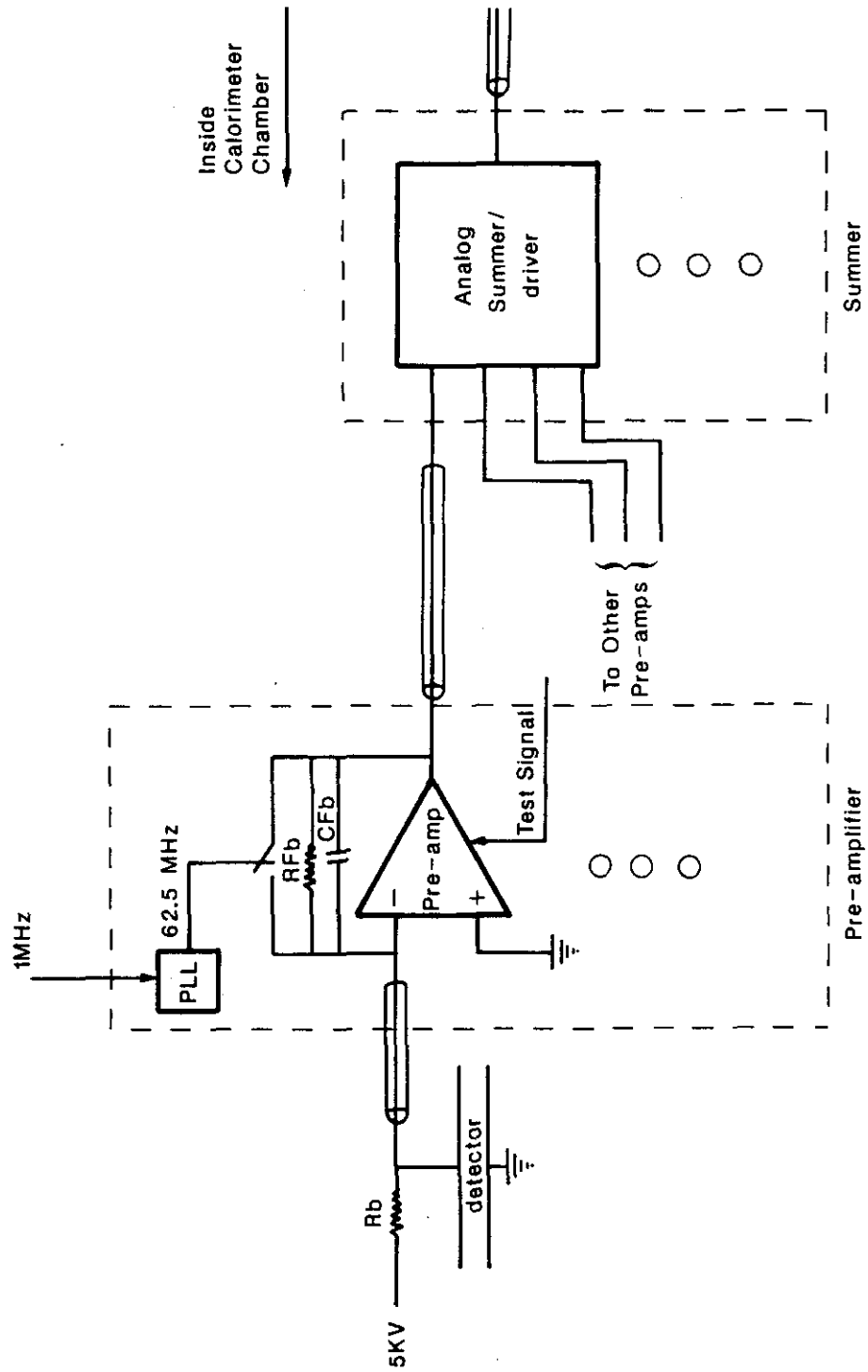


Figure 3 a). SSC warm liquid calorimetry front-end electronics.

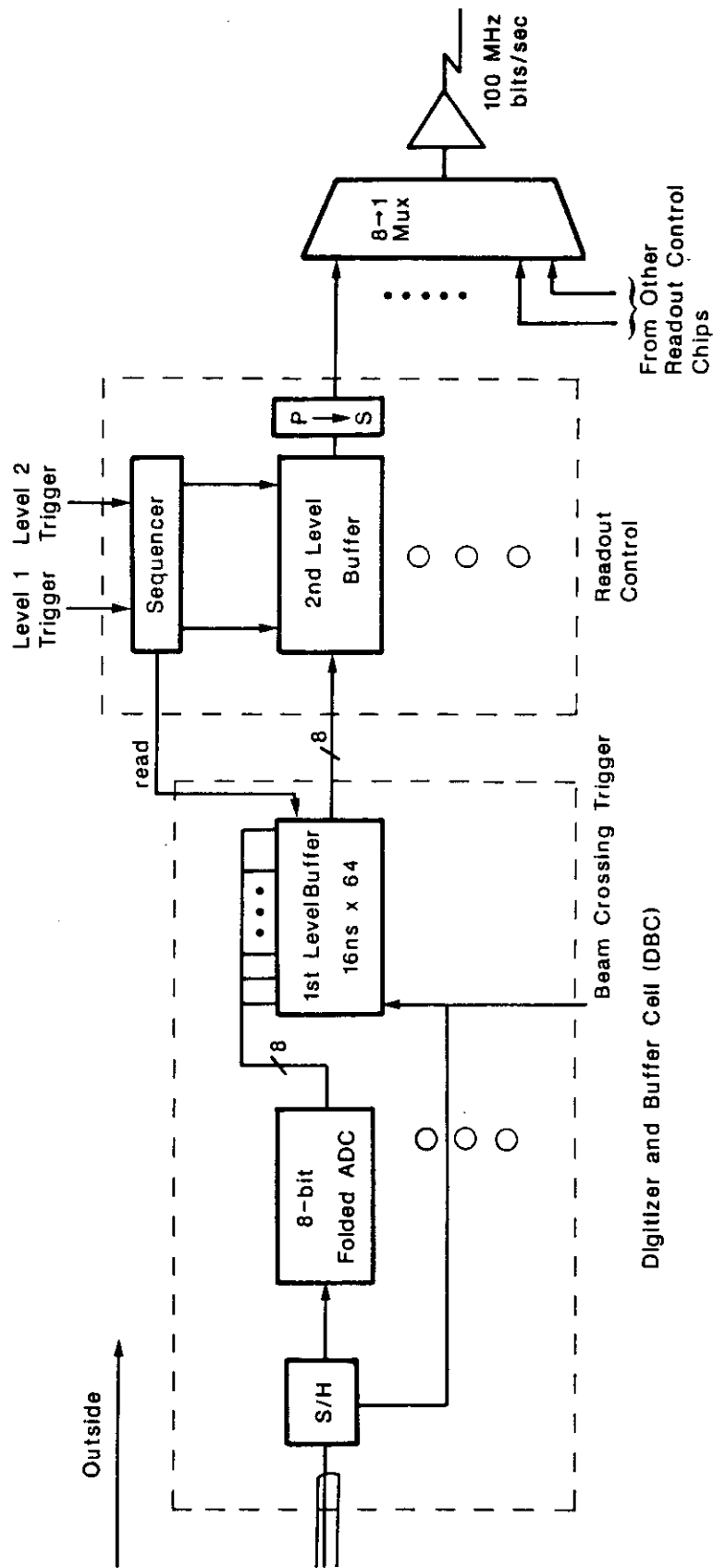


Figure 3 b). Digitizing, buffering, and readout electronics.

Preamplifier and Summer

Earlier calorimetry measurement systems have incorporated a charge-sensitive preamplifier as the first electronic device connected to the detector to amplify the signal to a level acceptable for commercially available electronic packages. Because the free electron drift time across the ionization gap of the detector cell is expected to be at least 3 to 4 times greater than the beam crossing time, it is very possible that single or multiple particle detections during successive beam crossings could saturate the preamplifier. A new preamplifier is proposed which will eliminate this problem. Results of SPICE simulation shown in Figure 4 indicate that the response of the present preamplifier design to the detector response⁶⁾ shown in Figure 5 is sensitive to the first part of the ionization charge across the detector cell. Accordingly, the original preamplifier design in Figure 6 is being modified so that a trigger signal near the end of the beam crossing interval will allow the preamplifier to discharge. Figure 7 shows a simulated detector response with a single particle detection at crossings i , $i+1$, and $i+2$ and 3 particles detected at crossing $i+7$. Figure 8 shows the response generated by the proposed preamplifier design.

Tests of earlier versions of the charge preamplifier of Figure 6 have shown a rise time of 37 nsec and a baseline noise level of less than 500 electrons rms. The 1 Grad radiation-hardened BiFET process by which the preamplifier in Figure 6 is being fabricated is expected to result in a factor of 3 to 4 improvement in rise time. Tradeoffs can be made to decrease rise time even further at the cost of increased noise. SPICE simulations, however, indicate that at the frequency of operation (62.5 MHz) flicker noise is a factor of 100 less than thermal noise with the present amplifier design. Design modifications can be made to reach a compromise between the two forms of noise to lower overall noise. Accordingly, the present preamplifier design is an excellent base on which to reach the proposed preamplifier. Table II lists the specifications expected of the proposed preamplifier. In addition, circuitry will be added to simulate an input charge equivalent to a single particle crossing to accommodate complete testing of the calorimetry measurement electronics.

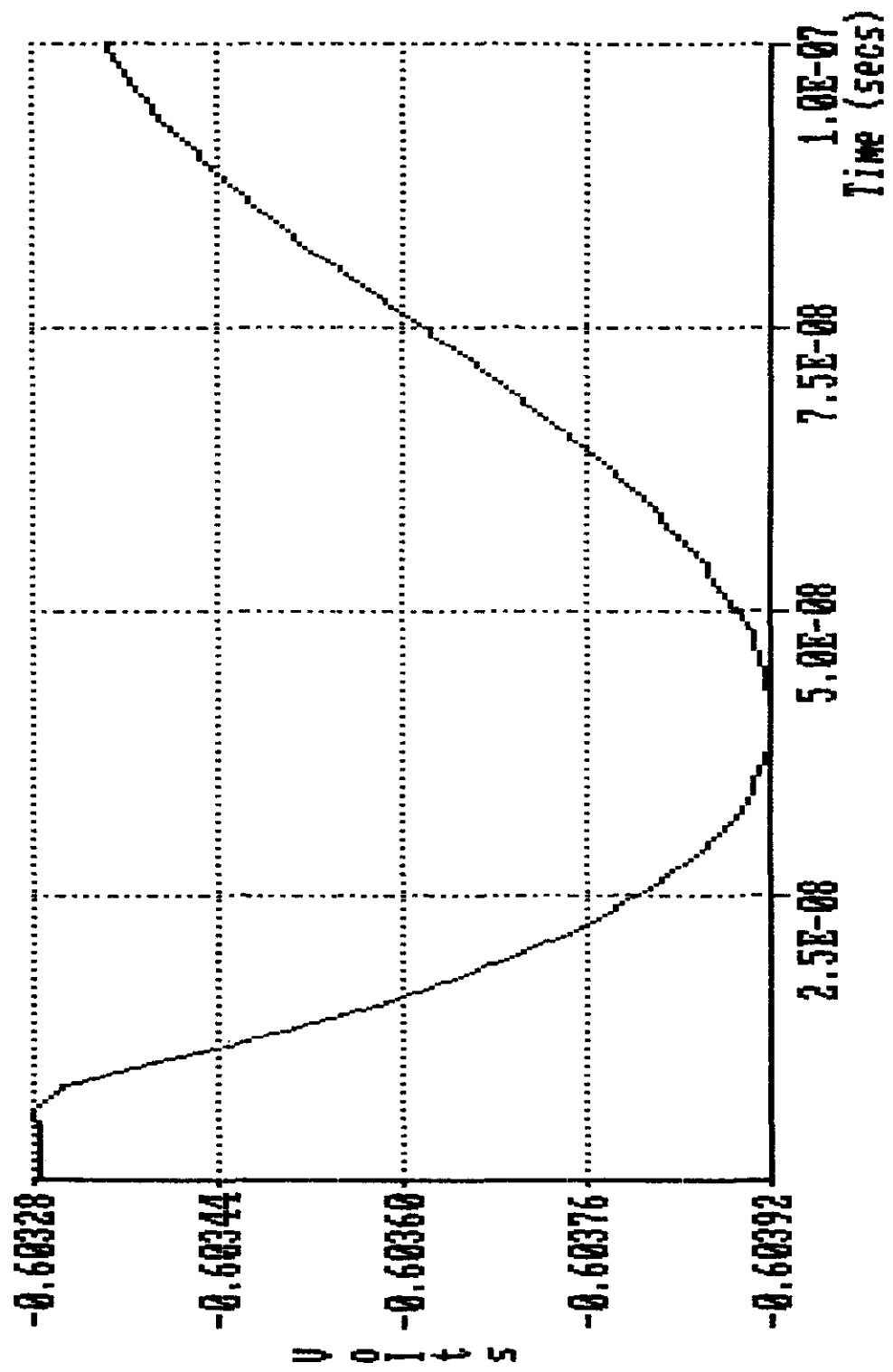


Figure 4. SPICE simulation showing preamplifier response to single particle crossing.

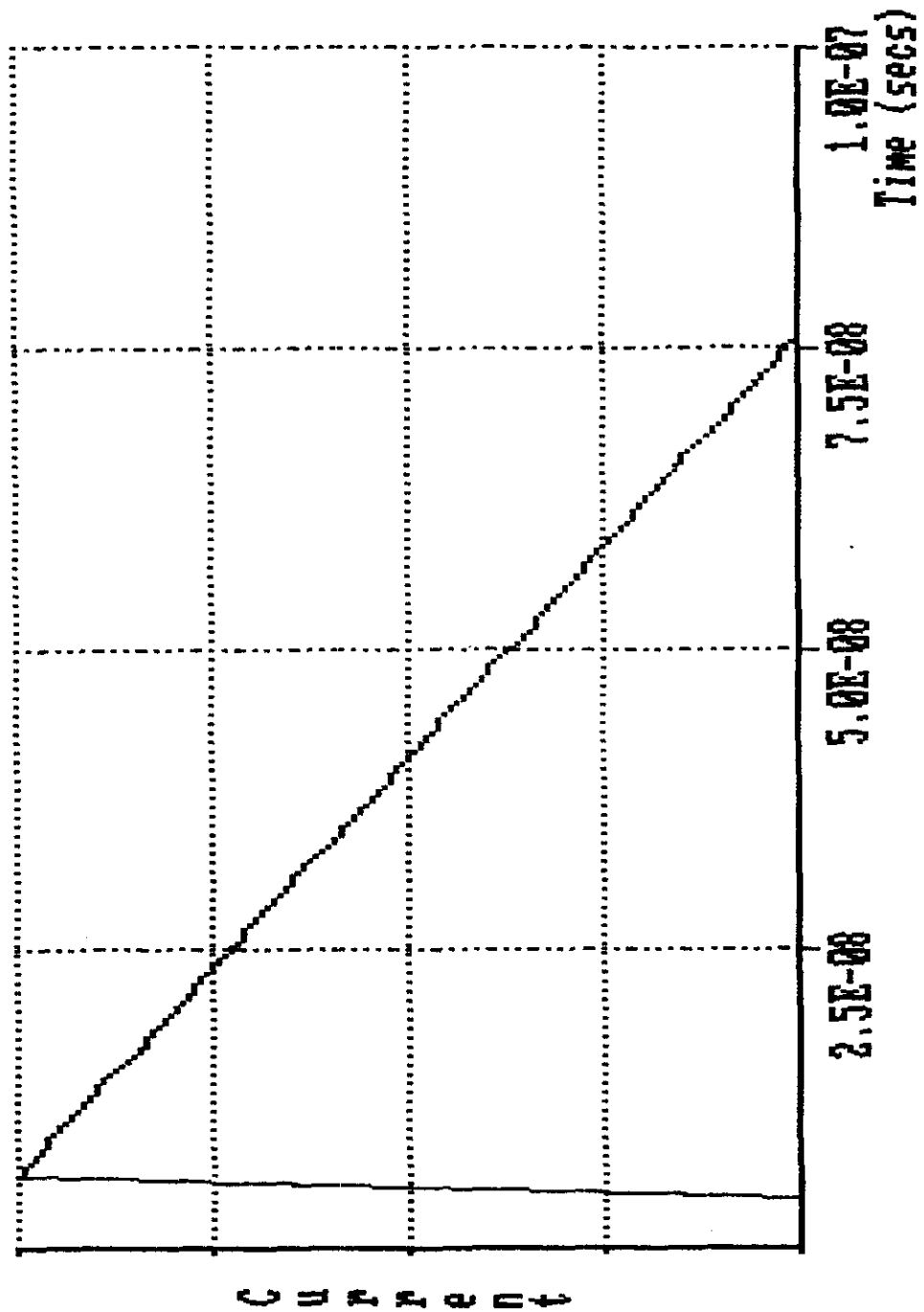
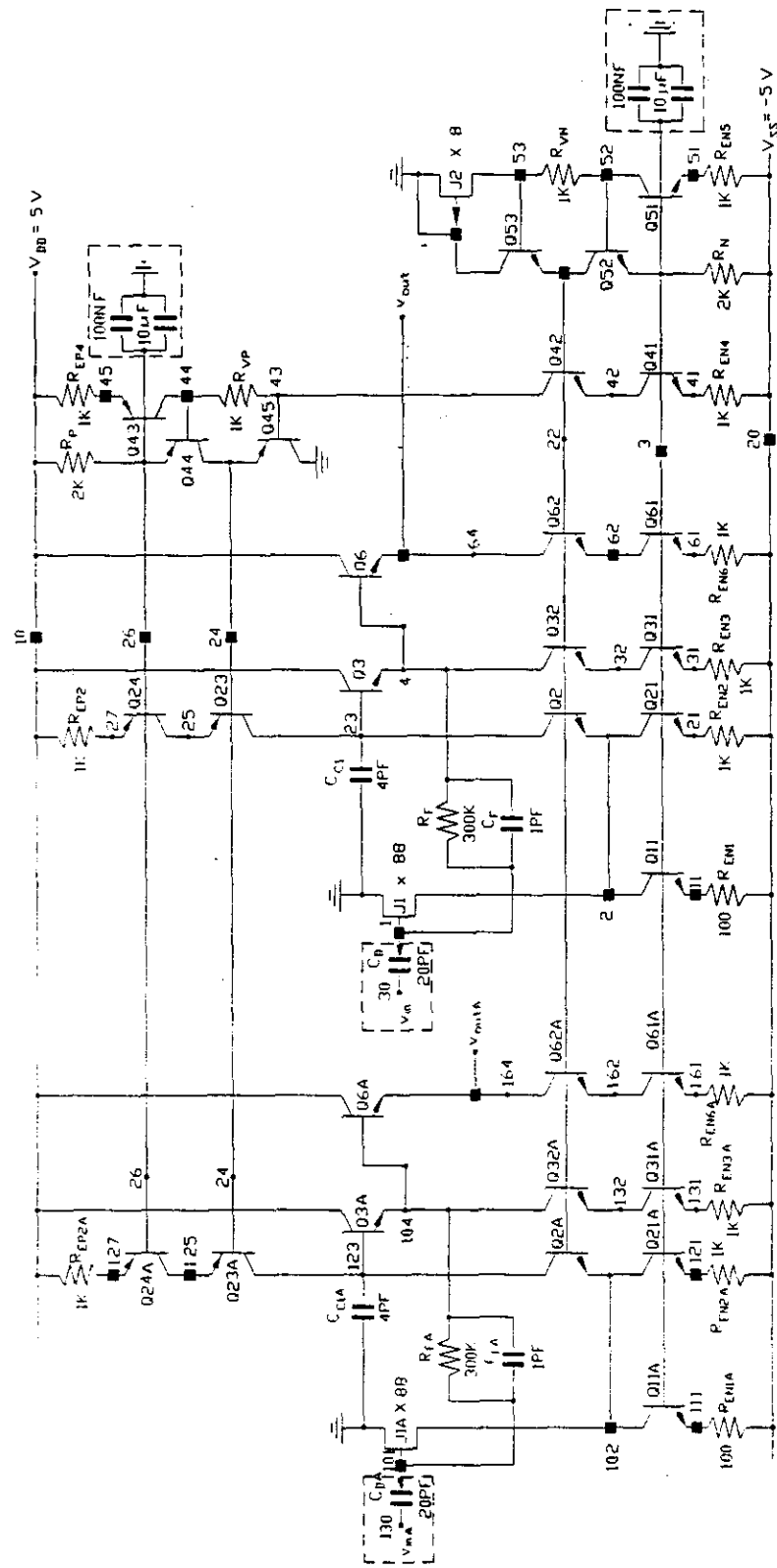


Figure 5. Detector response for single particle crossing (e^- drift = 75 nsec).



P.JET'S : = JB093S
 NPN'S : = NB101A X8
 PNP'S : = PB101A X8
 [] : = External Components
 [] : = Pads

Figure 6. Circuit schematic of charge preamplifier with reduced flicker noise.

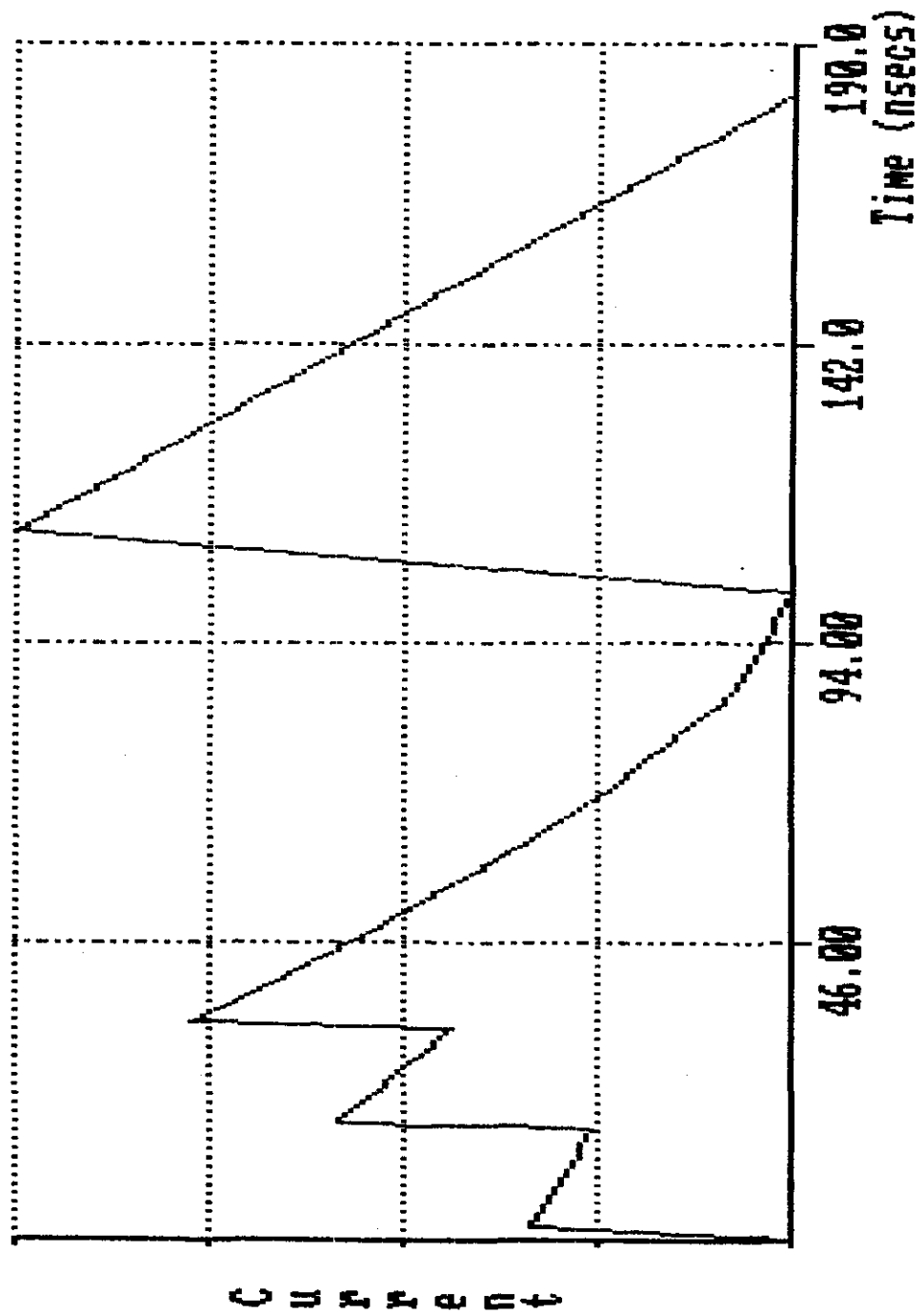


Figure 7. Detector current response within warm liquid cell for multiple particle crossings.

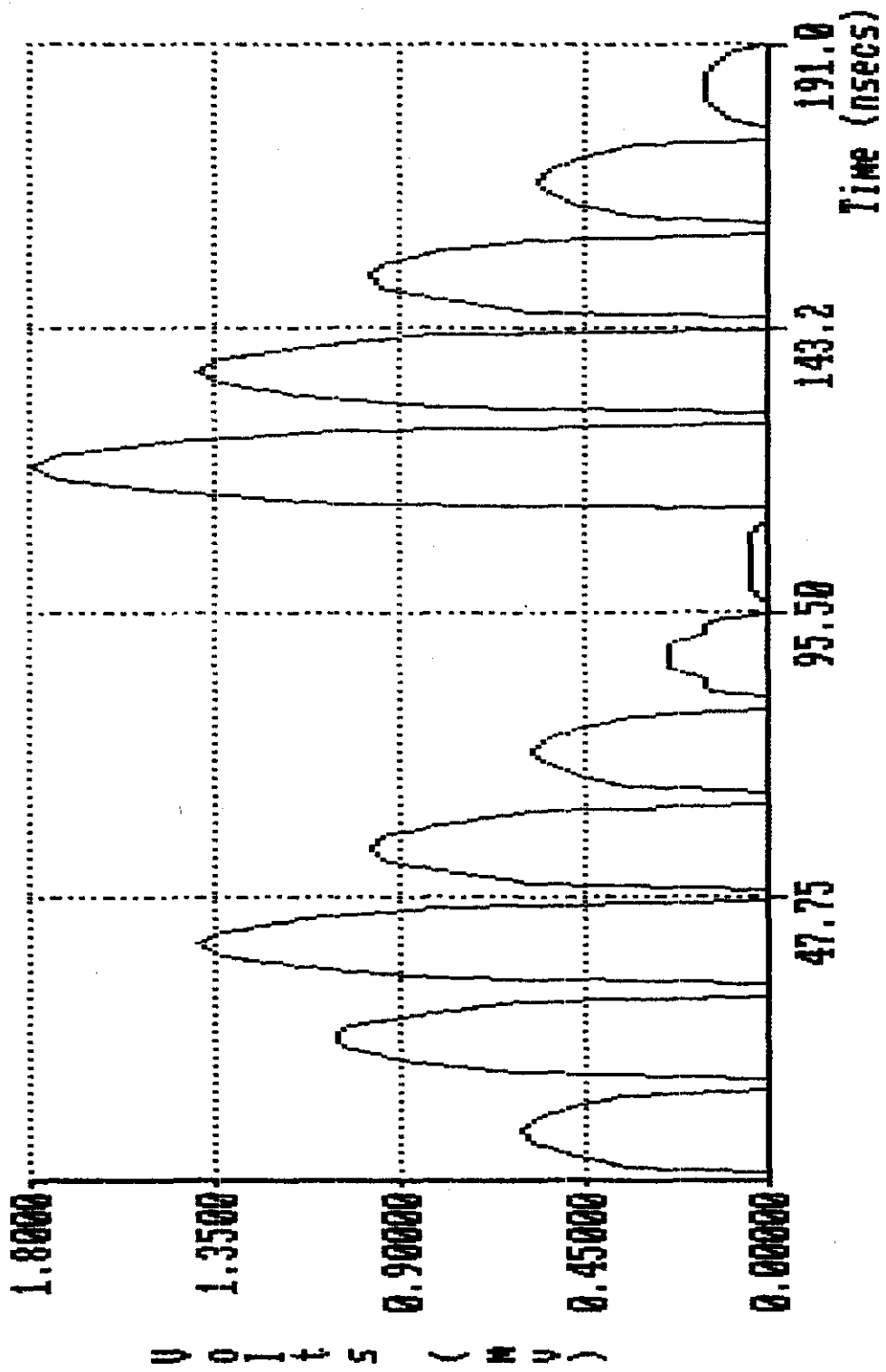


Figure 8. Charge preamplifier response to input signal of Figure 7.

The proposed summer circuit is a simple weighted summer configuration of the proposed low-noise charge preamplifier. Each summer will collect the outputs from at least four preamplifiers within a tower of detectors to result in a reduction in ADC component count by at least a factor of four. The summer chip will be located as close to respective preamplifiers as possible to reduce noise and, accordingly, is proposed for fabrication in the 1 Grad BiFET process provided by the Harris Semiconductor Corporation as the present charge preamplifier design.

Digitizer and Buffer Cell (DBC)

The output of each summer is connected to an eight-bit ADC. Expected timings in the SSC will require the high conversion performance of a flash or parallel architecture. An eight-bit flash converter, however, requires 255 comparators and will consume a lot of power and chip area. Such a design is unacceptable in the SSC. An alternative ADC is being designed based on a serial-parallel folded architecture shown in Figure 9. In general the conversion takes place during two periods of time. In the first period, a rough quantization is performed by a four-bit ADC and a digital-to-analog converter (DAC) settles to a final output value. In the second period, the quantized signal is subtracted from the sampled analog input signal and is applied to a second four-bit ADC for fine quantization to a digital signal. Figure 10 shows the proposed circuit design of the four-bit ADC. The proposed converter results in conversion performance similar to that of flash techniques^{16),17)}. However, circuit complexity and power dissipation are significantly reduced. Specifically only 24 comparators are required compared to the 255 comparators required for an eight-bit flash converter.

The proposed DBC includes enough buffer memory to store one μ sec of sampled data for first level triggering. The DBC and all electronics to follow will be located on the surface of the calorimeter detector system, outside the high radiation area. Accordingly, we propose to fabricate the DBC in a high-radiation CMOS technology to take advantage of the circuit density and low power requirements of CMOS technology. Up to eight ADC/memory channels and read/write circuits are planned per chip.

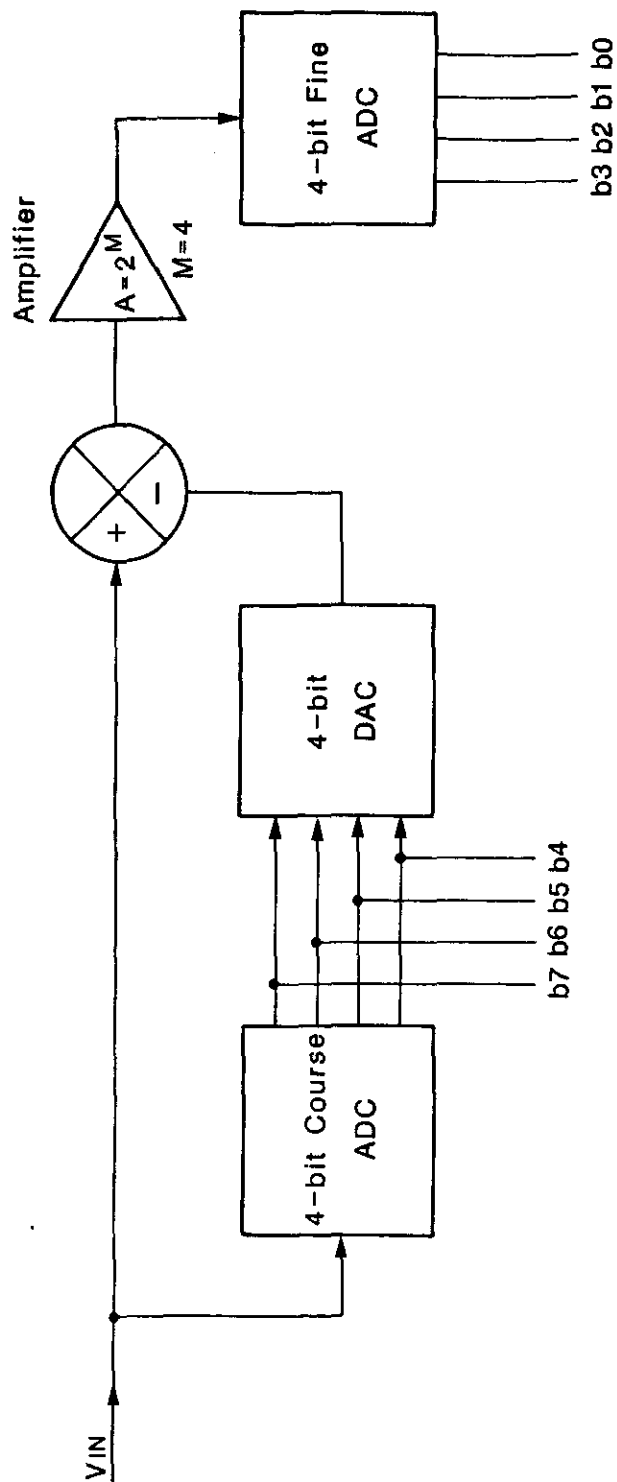


Figure 9. Proposed 8-bit Analog-to-Digital Converter.

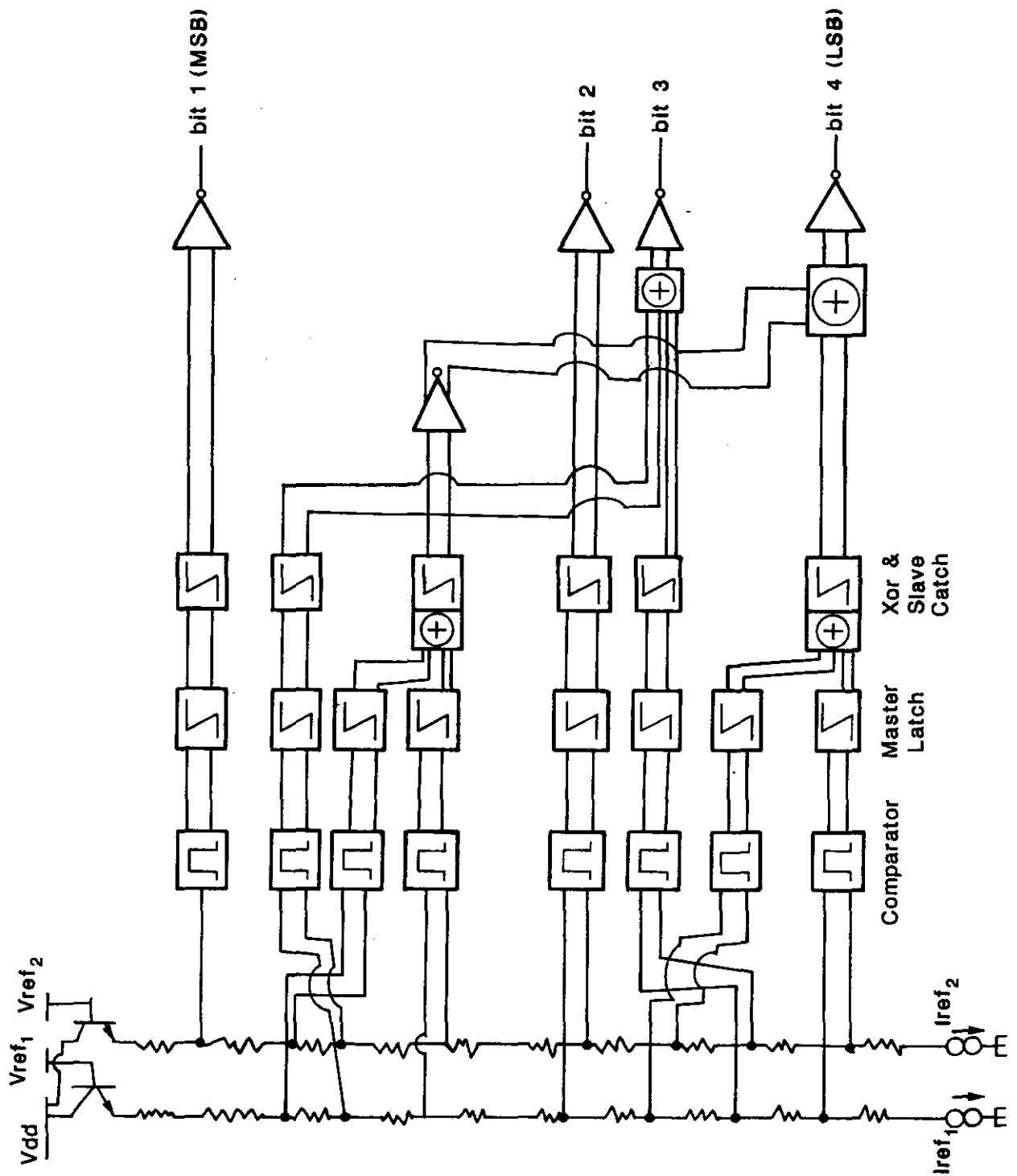


Figure 10. Proposed 4-bit Analog-to-Digital Converter.

Readout Electronics

Figure 11 shows the proposed electronics for the readout system. The readout control chip has a second level buffer, sequencers, and a parallel to serial converter. The second level buffer will be controlled by the level two readout sequencer which supports three pointers: write, read, and (multiple) trigger pointers. After the readout control chip receives a level two trigger, data is sent out through a parallel to serial converter to the control room. To transmit one μsec of recorded data, a single readout control chip will generate 4616 bits: $8 \text{ bits} * 64 \text{ columns} * 9 \text{ channels} + 8 \text{ bit column address}$. Eight readout control chips will be multiplexed to a single serial cable for a total of 36928 bits. If we assume a 100 Mbit/sec transmission rate, then 0.37 msec will be required to transmit one μsec of recorded data. Data compression schemes may be implemented to reduce the transmissions time. For the roughly 200,000 detector cells estimated for a typical hadron calorimeter, a maximum upper estimate of 50,000 ADC's will be required after summing in groups of at least four. In addition, 25,000 detectors will collect noise information which will require 6250 ADC's. With nine ADC's per DBC/readout control chip sets and multiplexing 8 chip sets per serial cable, 782 cables will be required to connect and transmit this data to the control room.

System Clock Distribution

Distribution of the 62.5 MHz beam crossing signal to all of the preamplifier chips will not be an easy task. Such a high frequency will be susceptible to external noise, phase shift due to cable impedance, etc. In order to maintain an acceptable level of clock synchronization throughout the system, a clocking scheme involving a Phase Lock Loop (PLL) located on each preamplifier chip is presently being designed. The noise power of the clock is proportional to frequency. Accordingly, by dividing the frequency of 62.5 MHz by 64, we can route a 1 MHz clock signal throughout the system and regenerate the beam crossing clock frequency locally via a PLL. Figure 12 shows the proposed system clock distribution system. The design of the appropriate PLL for this system can be found in the literature^{18),19)}.

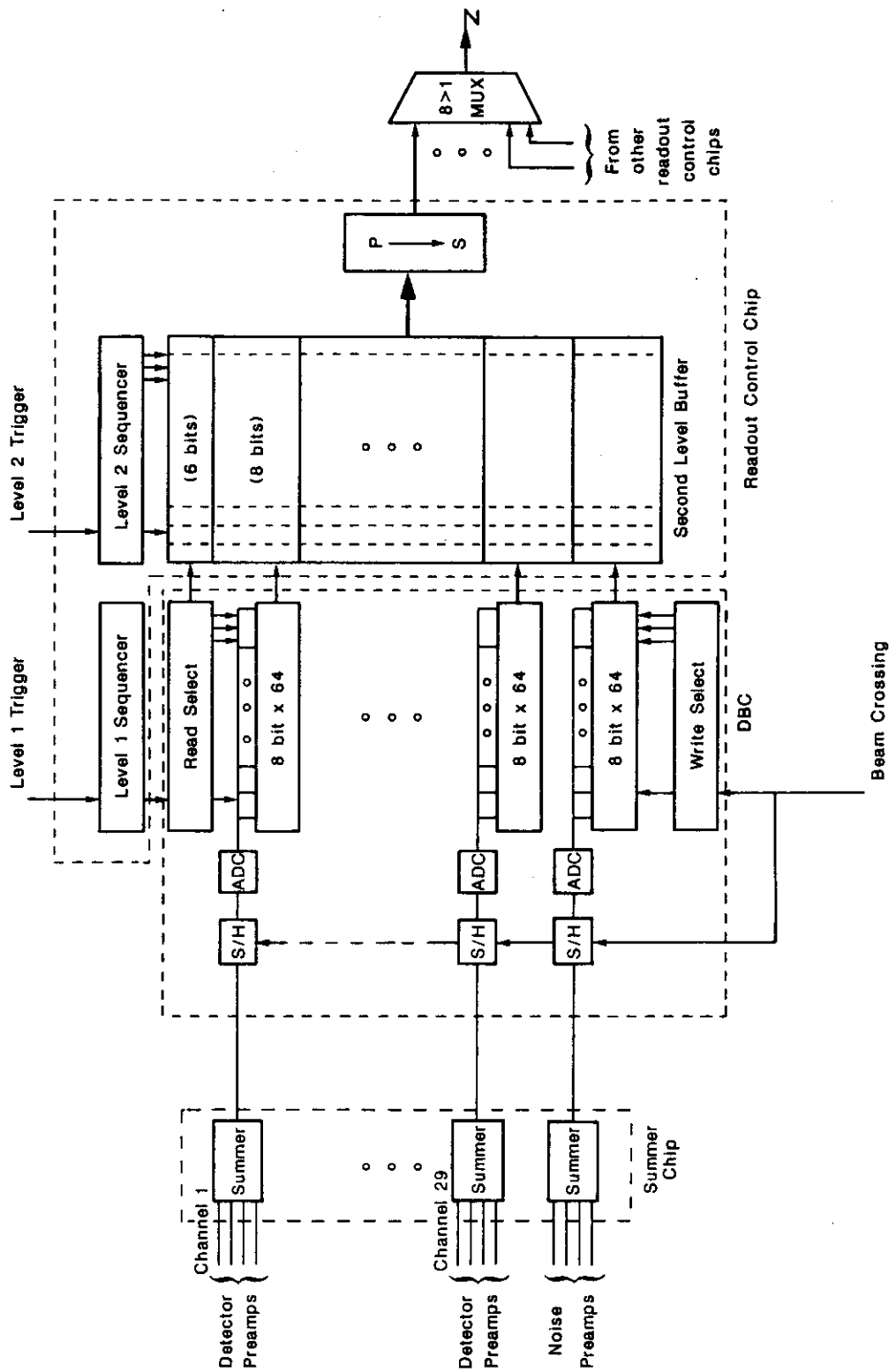


Figure 11. Readout control electronics.

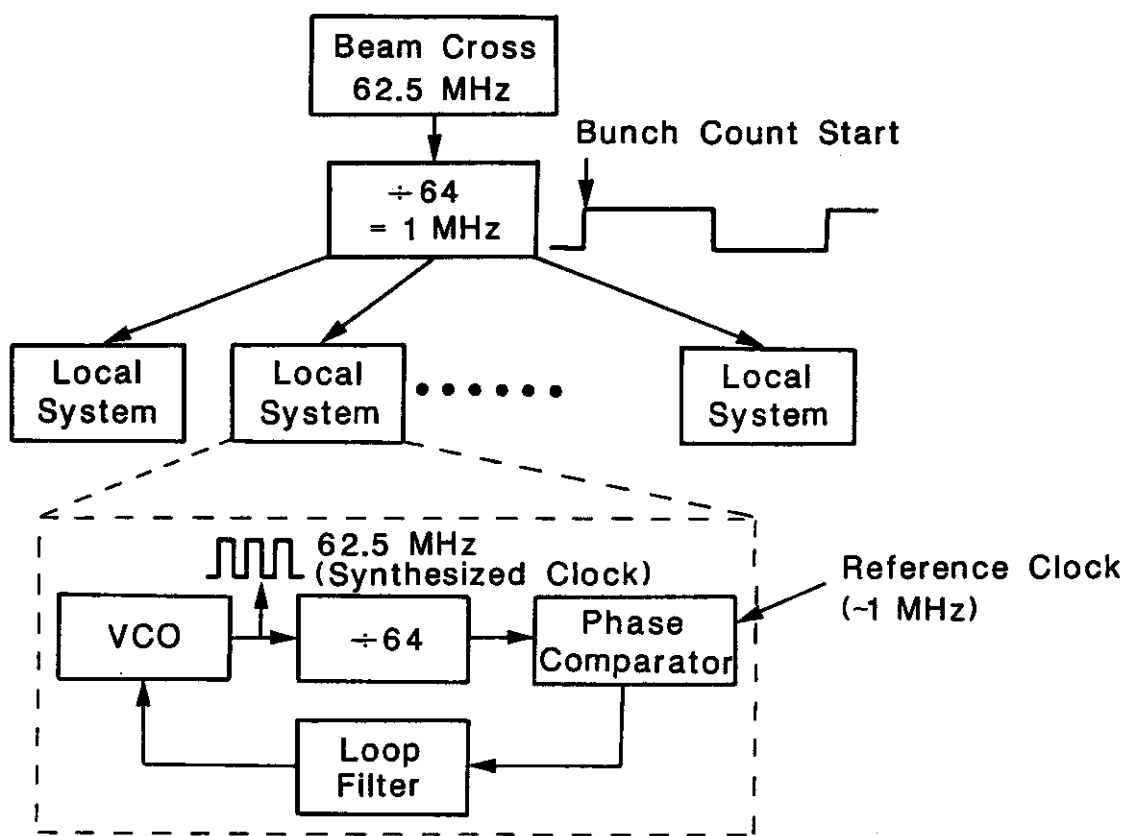


Figure 12. Proposed system clock distribution.

IV. R&D Manpower Commitments and Milestones

Faculty from the University of Alabama, Texas A&M University, the I. Physikalisches Institut der Rheinisch-Westfälischen Technischen Hochschule Aachen, and physicists from Oak Ridge National Laboratory and the Lawrence Berkeley Laboratory will be collaborating over a proposed two year period to develop a fast readout system for use in warm liquid calorimetry at the SSC. In addition to these research institutions, outside industrial engineers from Harris Semiconductor Corp., Hutchinson Technologies, Inc., and Coors Ceramics will be contributing to prototype construction of various components consisting of warm liquid cells and monolithic circuit implementation. The activities, manpower and estimated time scale, including milestones of the R&D, is described below.

Electronic Readout Subsystem

D. DiBitonto, L. Wurtz, and D. Mazumdar of the University of Alabama, together with P. Van Peteghem, K.-Y. Ling, H.C. Liu and S.Y. Lee of Texas A&M University will be responsible for the design and prototype evaluation of the 4-chip readout configuration described in section III. Facilities for circuit design and testing in the high energy physics group at the University of Alabama included a newly commissioned VLSI evaluation laboratory shown in Figure 13, Apollo workstations that will support the Mentor Graphics software design package, and access to the Alabama Supercomputing Network in Huntsville, Al. for circuit simulation. Thanks to an ongoing R&D program of VLSI design and evaluation in radiation-hardened monolithic BiFET and CMOS technology with Texas Instruments and Harris Semiconductor Corp., we are presently submitting circuit designs to these corporations for monolithic implementation at no charge to us (see Appendix I).

We expect to have the complete system designed and simulated by the end of this year, based on preliminary semiconductor device specification technology from the IC manufacturer. Once a design is ready to be submitted for monolithic implementation, approximately 6 months will be required for these manufacturers to provide us the first prototype chips for testing here at the University of Alabama.

THE UNIVERSITY OF ALABAMA

HIGH-ENERGY PHYSICS LAB

VLSI EVALUATION SYSTEM



8 MB

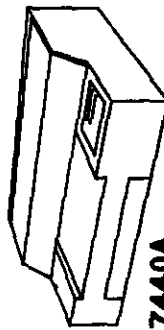
323 MB

APPLICATIONS:

HP-UX

C, HP-BASIC/UX

INTERACTIVE TEST GENERATOR



7440A
PLOTTER

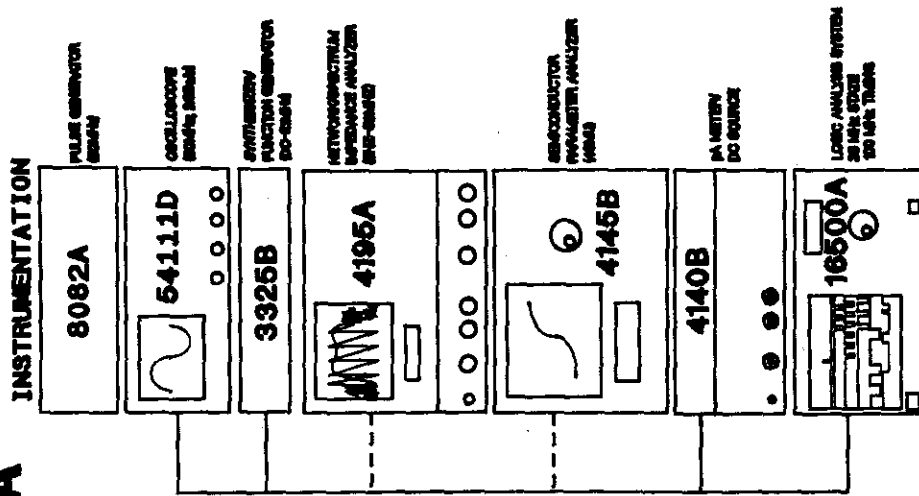
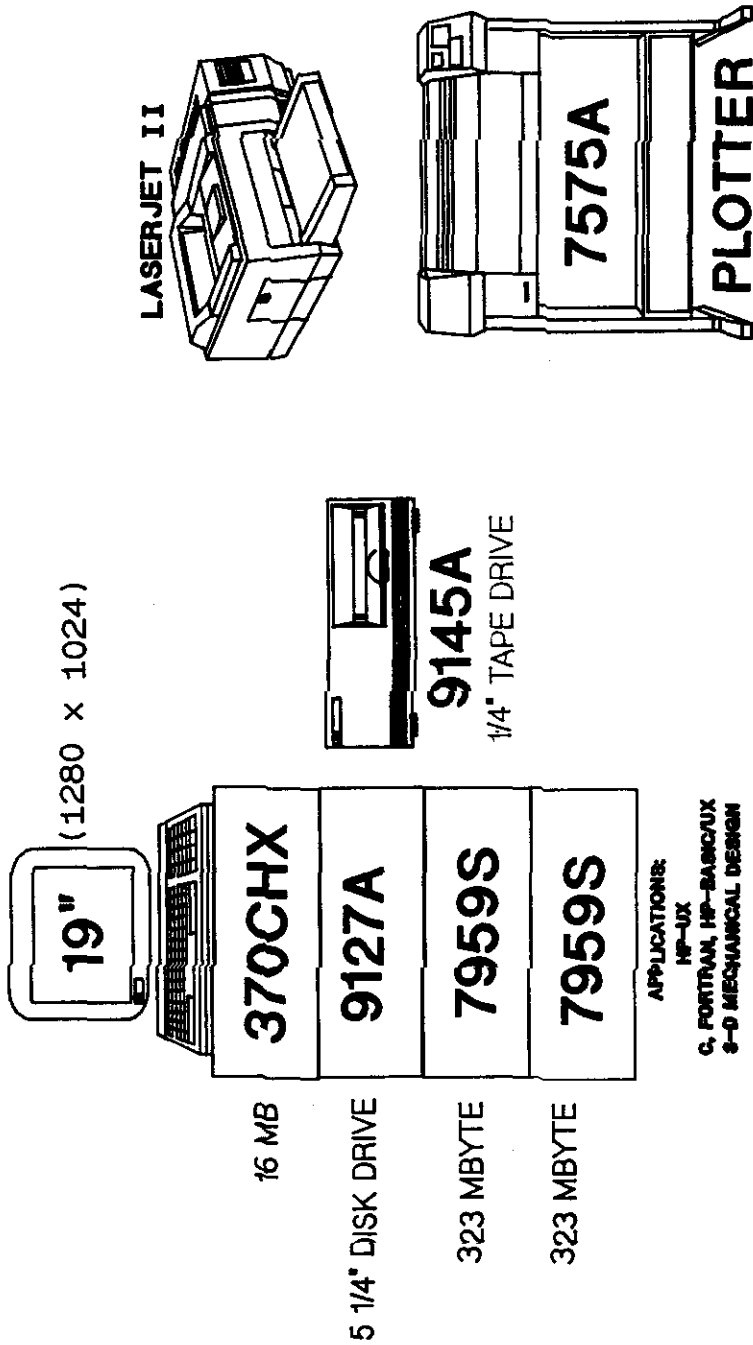


Figure 13 a). The University of Alabama VLSI Evaluation Laboratory.

THE UNIVERSITY OF ALABAMA

HIGH-ENERGY PHYSICS LAB

COMPUTER AIDED DESIGN SYSTEM



APPLICATIONS:
HP-UX
C, FORTRAN, HP-BASIC/UX
8-D MECHANICAL DESIGN



Figure 13 b). Graphic Design Support Facility.

When these prototype circuits have been successfully tested, an additional production run of 50-100 channels to instrument a full representative calorimeter tower will take an additional 6-9 months to complete. This increase is due to the production scheduling within the industrial manufacturer for non-prototype fabrication. By that time prototype warm liquid cells already under construction should be ready to be equipped with the readout electronics.

Detector Design Simulation

J. Busenitz, D. DiBitonto, and Y.-Y. Wu of the University of Alabama and T. Gabriel, B. Bishop, and P. Fu of Oak Ridge National Laboratory will be responsible for simulating the detector response with CALOR89 and other Monte Carlo codes (GEANT, ISAJET). Computational facilities available in the high energy physics group will include an Apollo DN-10,000 with a 16 mips parallel processor, a University IBM 3090, and access to the Alabama Supercomputer Network. To accommodate more general physics issues such as hermiticity, acceptance, and overall detector response to larger design constraints, K. Lübelmeyer and K. Genius of the I. Aachen Technical Institute will be providing us with engineering design input of a larger, more complete hadron calorimeter for our Monte Carlo simulation studies.

Code implementation and simulation here at the University of Alabama should be ready in 3-6 months time. The CALOR89 code, which is presently operational at ORNL, will eventually be installed and run here at Alabama with the help of T. Gabriel and collaborators.

Prototype Warm Liquid Cells

Prototype warm liquid cells designed for fast output response are presently being built by Coors Ceramics and Hutchinson Technologies (see Appendix II). D. DiBitonto, J. Busenitz and M. Timko are presently responsible for the assembly and testing of these devices at the University of Alabama and at the MT test beam facility at Fermilab (already approved and scheduled to begin tests on the fundamental properties of warm liquids). Two prototype cells are expected to be ready for testing in October, after which time an order to instrument a complete tower

based on this design is ready to be submitted. Due to the small volumetric size of each prototype cell, the WALIC Collaboration of the Lawrence Berkeley Laboratory has offered to fill our vessels free of charge as they come off the Hutchinson Technology Production line. Once tests have been completed on the first two cells, a production run to make 50 of these cells is expected to take 6-9 months, due to scheduling of present vessel manufacture.

Test Beam Requirements

A test beam program to measure the fundamental properties of warm liquids has already been approved and is presently being prepared by the WALIC Collaboration in the Fermilab MT test beam area. Due to the small, compact size of our prototype detector, this device can easily be placed in this test beam with little or no disturbance to the ongoing measurement program already planned in this area. The proposed readout system is sufficiently integrated to be read out with portable (HP) test equipment presently being developed here at the University of Alabama.

V. Budget Justification

The budget detail for the proposed R&D program for FY90 is given on page 33 of this proposal. The actual R&D activity in this program is proposed over a 3-year period. We are requesting summer salary support for three faculty members, in addition to one full-time postdoctoral research physicist, Dr. Mark Timko. Summer salary support is also requested for three senior staff physicists from Oak Ridge National Laboratory to implement and run detector simulation code. Support is also requested for three full-time graduate students to help with the project. A travel budget category is included to attend scientific meetings and coordinate test beam work expected at Fermilab.

We are also requesting capital equipment funds to build and instrument a representative warm liquid "tower" complete with the proposed fast readout system. Although single channel prototyping will be done at no charge to us, a series production run of 50-100 channels will include the cost of metal masking (\approx \$25,000).

We estimate that the cost of the charge preamplifier will be \$40 per channel. The cost for the summer, digitizer, and buffer cells are expected to be in the same price range as the preamplifier, with the exception that they will serve at least four detector channels. The total cost per channel is then estimated to be \approx \$70. The cost to produce a 16 channel electrode is \$1,035 (\$300 for a laser welded and surface cleaned vessel from Hutchinson Technologies, Inc., and \$735 for the ceramic electrode from Coors Cermamics). Other direct costs include the manufacture and testing of support electronics, materials and supplies, and communication/publication charges.

References

1. R. Holroyd, "Effects of Radiation Damage to TMP, TMS, and Liquid Argon Solutions," SSC-SR-1035, p. 335, June, 1988.
2. D. Groom, "Radiation Levels in the SSC Interaction Regions," SSC-SR-1033, June 10, 1988;

D. Groom, "Radiation Levels in SSC Calorimetry," Proceedings of the Workshop on Calorimetry for the SSC, Tuscaloosa, Alabama, March 13-17, 1989.
3. R. Wigmans, "The Spaghetti Calorimeter," Proceedings of the Workshop on Calorimetry for the SSC, Tuscaloosa, Alabama, March 13-17, 1989.
4. M.G. Albrow et al., "Performance of a Uranium/Tetramethylpentane Electromagnetic Calorimeter," Nucl. Instr. and Meth. in Phys. Research **A265** (1988) 303.
5. D. DiBitonto et al., "Integrated Ceramic Electrode for Warm Liquid Calorimetry," Proceedings of the Workshop on Calorimetry for the SSC, Tuscaloosa, Alabama, March 13-17, 1989.
6. V. Radeka, "Electronics Considerations for SSC Calorimetry," Proceedings of the Workshop on Calorimetry for the SSC, Tuscaloosa, Alabama, March 13-17, 1989.
7. W.J. Willis and V. Radeka, "Liquid-Argon Ionization Chambers as Total-Absorption Detectors," Nucl. Instr. and Meth. **120** (1974) 221.
8. D. DiBitonto et al., "Advanced Forward Calorimetry for the SSC and TeVatron Collider," Nucl. Instr. and Meth. in Phys. Research **A279** (1989) 100.
9. D. DiBitonto et al., "Fast, Radiation-Hard Charge Preamplifier for Warm Liquid Calorimetry," Proceedings of the Workshop on Calorimetry for the SSC, Tuscaloosa, Alabama, March 13-17, 1989.
10. D. DiBitonto et al., "Annual Report and Renewal Proposal: SSC Generic Detector R&D," May 1989, submitted to the U.S. Department of Energy, SSC Division.
11. See "Review of Particle Properties," Physics Letters **B204** April 1988.

12. K. Lübelsmeyer, "Concept for the Design and Assembly of a Hadron Calorimeter for a Collider Experiment," I. Physikalisches Institut der Rheinisch-Westfälischen Technischen Hochschule Aachen, June 14, 1989, Aachen, Germany.
13. A. Matsuzawa, "200 MSPS 8b A/D Converter with a duplex gray coding," Dig. of Tech. Papers, Symposium on VLSI Circuits, May 1987.
14. C. Clayton, "FFT performance testing of data acquisition systems containing buffer, A/D converters, and S/H circuits," IEEE T. Instrumentation and Measurement, pp 212-215, June 1986.
15. S. Lewis and P. Gray, "Circuit techniques for monolithic CMOS video A/D Conversion," ISSCC Dig. of Tech. Papers, May 1987.
16. R. Van de Plassche and P. Baltus, "An 8b, 100 MHz A/D Converter with 500 MHz Resolution Bandwidth," ISSCC Dig. of Tech Papers, Feb. 1988;
17. Y. Yoshi et al., "8b 350 MHz flash ADC," ISSCC Dig. of Tech. Papers, Feb. 1987.
18. E. Murthi, "A Monolithic Phase-locked loop with Post Detection Processor," IEEE J. of Solid-state Circuits, Vol SC-14, No. 1, February 1979;
19. R.R. Cordell and W.G. Garret, "A highly stable VCO for application in monolithic phase-locked loops," IEEE J. Solid-state Circuits, Vol SC-10, pp 480-485, Dec. 1985.

Table I

Hadron Calorimeter Mechanical Specifications

Bending Moment Resp. Calorimeter Weight	$M = 1000 \times 3 \text{ tons}$ $= 3 \times 10^{10} \text{ Nmm}$
Moment of Inertia (Wall Thickness $D = 20 \text{ mm}$)	$W = (\pi/32D)(6000^4 - 5960^4)$ $= 5.6 \times 10^8 \text{ mm}^3$
Bending Stress in Walls	$\sigma = 53 \text{ N/mm}^2$
Longitudinal Segmentation	100 - 123 samples

Table II

Electronic Specifications of Proposed Preamplifier

Sensitivity	$1\text{V/pC} = 0.64\text{mV}/4000\text{e}^-$
Noise	$1000\text{e}^- \text{ rms}$
Risetime	$\approx 5\text{ nsec}$
Fall time after trigger	$\approx 5\text{ nsec}$
Bandwidth	$\approx 100\text{ MHz}$
Power Dissipation	60 mW/channel
Linearity	$\leq 0.1\%$
Variation over Temp. and Supply Range	$\leq 0.5\%$
Technology	BiFET
Radiation Hardening	1 Grad
Estimated Cost	$\approx \$40/\text{channel}$

Proposed Budget for SSC Subsystem R&D

Proposed Funding Period: 01/01/90 - 12/31/91

FY 1990

A. Senior Personnel

D. D. DiBitonto

3 Summer Months/Year

\$17,400

B. Other Personnel

1. Assistant Professor of Physics

Dr. Jerome Busenitz

3 Summer Months/Year

\$10,667

2. Assistant Professor of Electrical Engineering

Dr. Larry Wurtz

3 Summer Months/Year

\$13,667

3. Assistant Research Scientist

Dr. Mark Timko

12 Calendar Months/Year

\$30,000

4. Senior Oak Ridge Laboratory Staff

Dr. Tony Gabriel

Dr. Barbara Bishop

Dr. Peter Fu

3 Summer Months/Year

\$42,500

5. 3 Full-time Graduate Research Assistants

(D. Mazumdar, S.L. Sledge, and Y.-Y. Wu)

12 Calendar Months/Year

\$37,800

FY 1990

C. Fringe Benefits

FICA and Insurance (22% of A, B.1, B.2 and 29% of B.3)	\$17,881
Total Salaries, Wages and Fringe Benefits	\$169,915

D. Capital Equipment

50 warm liquid modules, with monolithic readout electronics	\$75,000
--	-----------------

E. Other Direct Costs

1. Manufacturing of PC mother boards, preparation of measurements	\$2,500
2. Engineering Circuit Design	\$2,000
3. Materials and Supplies	\$2,500
4. Shop time (@ \$6.00/hr)	\$1,500
5. Communications	\$500
6. Publication Charges	\$500
Subtotal	\$9,500

	<u>FY 1990</u>
F. Travel	
1. Domestic (12 trips to Fermilab, and to attend scientific meetings)	\$7,000
2. Foreign (4 Foreign scientific meetings)	\$5,000
Total Travel	\$12,000
 G. Total Direct Costs	 \$266,415
 H. Indirect Costs	
@ 46% of Modified Total Direct Costs	\$68,501
 I. Total Direct and Indirect Costs	 \$334,916

Appendicies

- I. "Fast, Radiation-Hard Charge Preamplifier for Warm Liquid Calorimetry," Proceedings of the Workshop on Calorimetry for the SSC, Tuscaloosa, Alabama, March 13-17, 1989.

- II. "Integrated Ceramic Electrode for Warm Liquid Calorimetry," Proceedings of the Workshop on Calorimetry for the SSC, Tuscaloosa, Alabama, March 13-17, 1989.

Fast, Radiation-Hard Charge Preamplifier for Warm Liquid Calorimetry

D. DiBitonto, S. Narayan, P.M. VanPeteghem,
S.-Y. Lee, K.-Y. Ling, and H.-C. Liu

Texas A&M University
College Station, Texas

Abstract

We describe the design, construction, and operation of an ultra-sensitive, high-bandwidth charge preamplifier for calorimetry at the Superconducting Super Collider. The design is based on a monolithic, bipolar technology with 5 Mrad radiation hardness. The intrinsic low noise ($\leq 600 e^-$ rms) and low power consumption (60 mwatt) of this device at room temperature make it an attractive front-end preamp for either warm or cryogenic liquid media detectors, or even for tetrodes for scintillating fiber technology. Measurements are reported on a prototype device built in an industrial BiFET process with a 37 nsec risetime.

Workshop on Calorimetry for the Superconducting Super Collider
Tuscaloosa, Alabama, March 13-17, 1989

I Introduction

In a previous paper¹⁾ we described the design and construction of a warm liquid ionization cell to instrument the very forward collider region. Here we describe the front-end charge preamplifier which has been designed for this particular application. Due to the very severe constraints of radiation hardness²⁾, speed, and sensitivity on the electronics³⁾ in this region, we have investigated a design based on monolithic, bipolar technology with 5 Mrad radiation hardness. Radiation hardness up to 1 Grad is presently available in the same technology⁴⁾, although this technology far exceeds the requirements of an SSC application even in the most extreme cases.

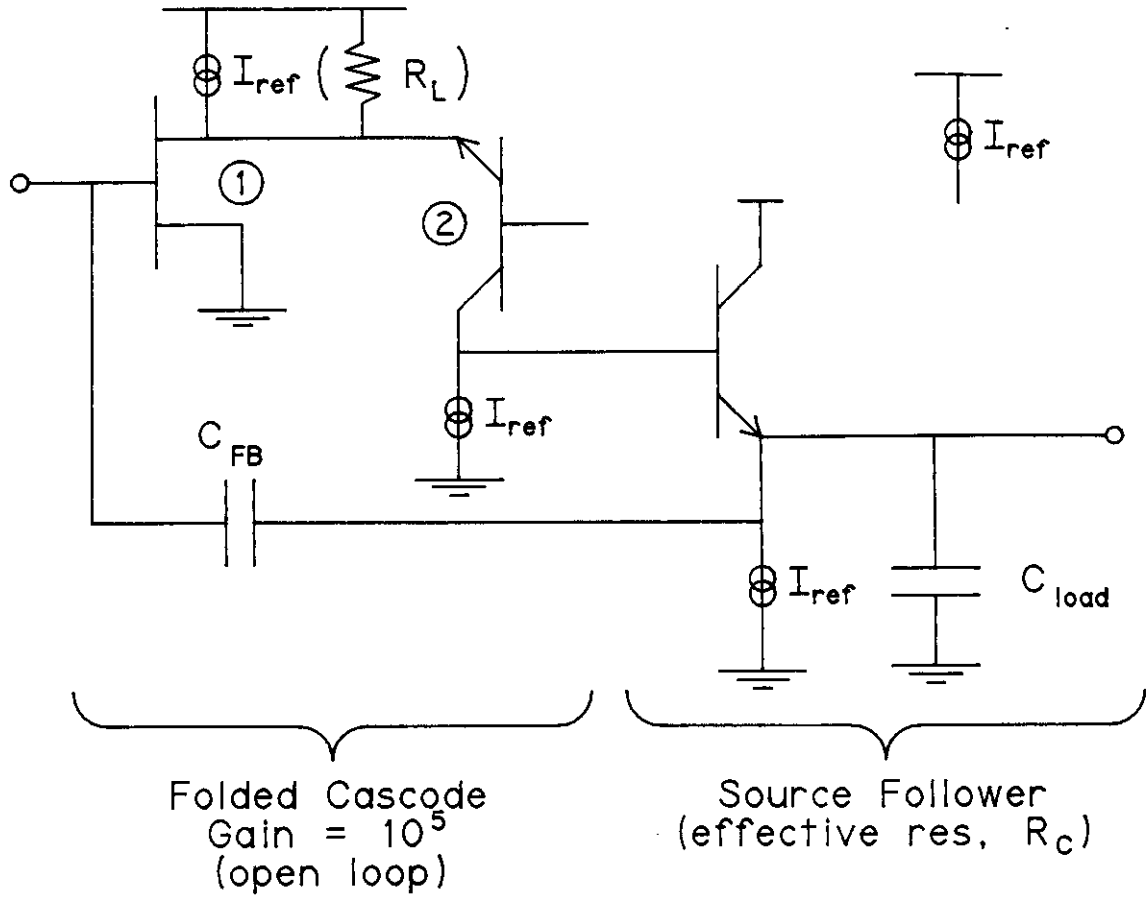
Detector capacitance is crucial in matching detector response to the high accelerator bandwidths expected at the SSC. In the particular application of a small angle calorimeter¹⁾, the maximum free electron drift time within this cell can be as fast as 50 nsec⁵⁾. Although the free electron drift time across these ionization gaps is not affected by detector capacitance, the response time and noise of a front-end charge preamplifier certainly are. We have taken the approach to minimize the effects of potentially high capacitive loads and long readout cables by designing an amplifier which will operate **directly on** the detector itself with typically less than 100pF of input source capacitance¹⁾.

Similar charge preamplifier designs based on gallium arsenide technology are presently being investigated within our group. Although this technology has a much higher radiation hardness than that of bipolar, gallium arsenide is still a very emerging technology.

II Design and Simulation

The SPICE analogue circuit simulation program was used to simulate and optimize the BiFET circuit⁶⁾ shown schematically in Figure 1. This basic circuit consists of a folded cascode arrangement with a p-type JFET input device and a source follower output stage. The actual circuit design submitted to Texas Instruments is shown in Figure 2, complete with biasing and current mirrors. Note that the feedback capacitance in this design is 1 pF. The corresponding feedback resistance of 10 G Ω can be reduced for shorter settling times, depending on the desired dc operating output level in high rate operation.

BASIC CIRCUIT



Transconductance: $(g_m)_1 = \sqrt{2 I_{bias} \frac{kW}{L}}$

k = "transconductance parameter"
 related to mobility
 W, L = width, length

$$(g_m)_2 = \frac{q I_c}{kT} \left[\frac{I}{V} \right]$$

$$G_{TOT} = (g_m)_1 R_L (g_m)_2 R_C$$

Fig. 1 Basic schematic of the BiFET charge preamplifier.

HIGH SPEED CHARGE PREAMP

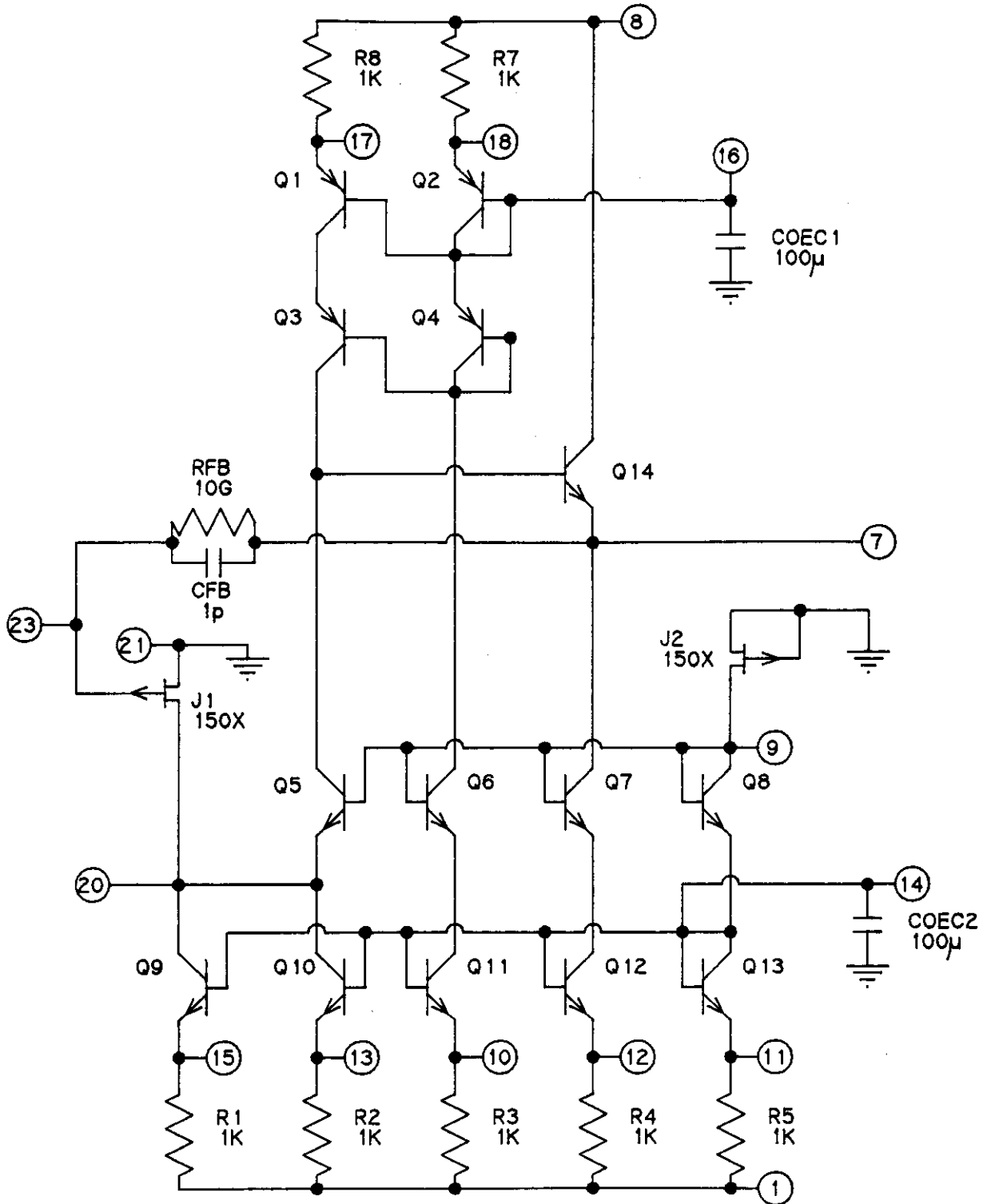
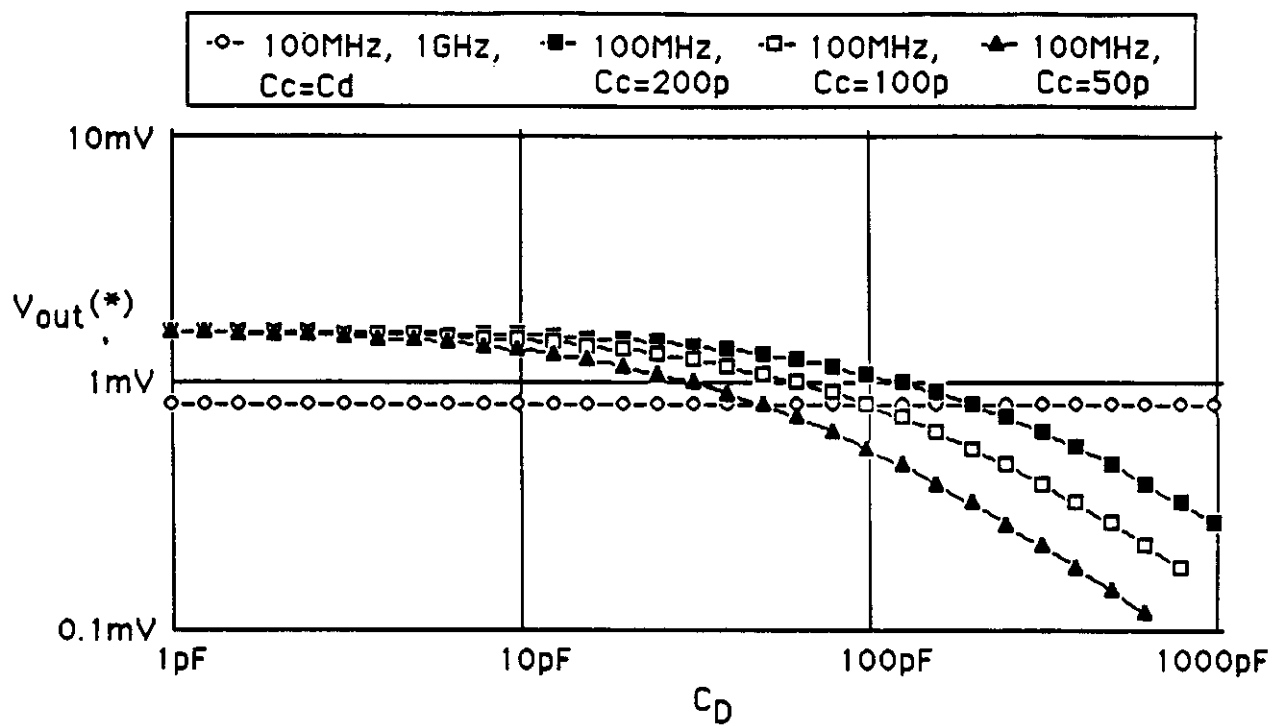


Fig. 2 Complete schematic of the BiFET charge preamplifier.



(*) For 10,000 Electrons input charge

Fig. 3 Output voltage versus detector capacitance for varous values of decoupling capacitance.

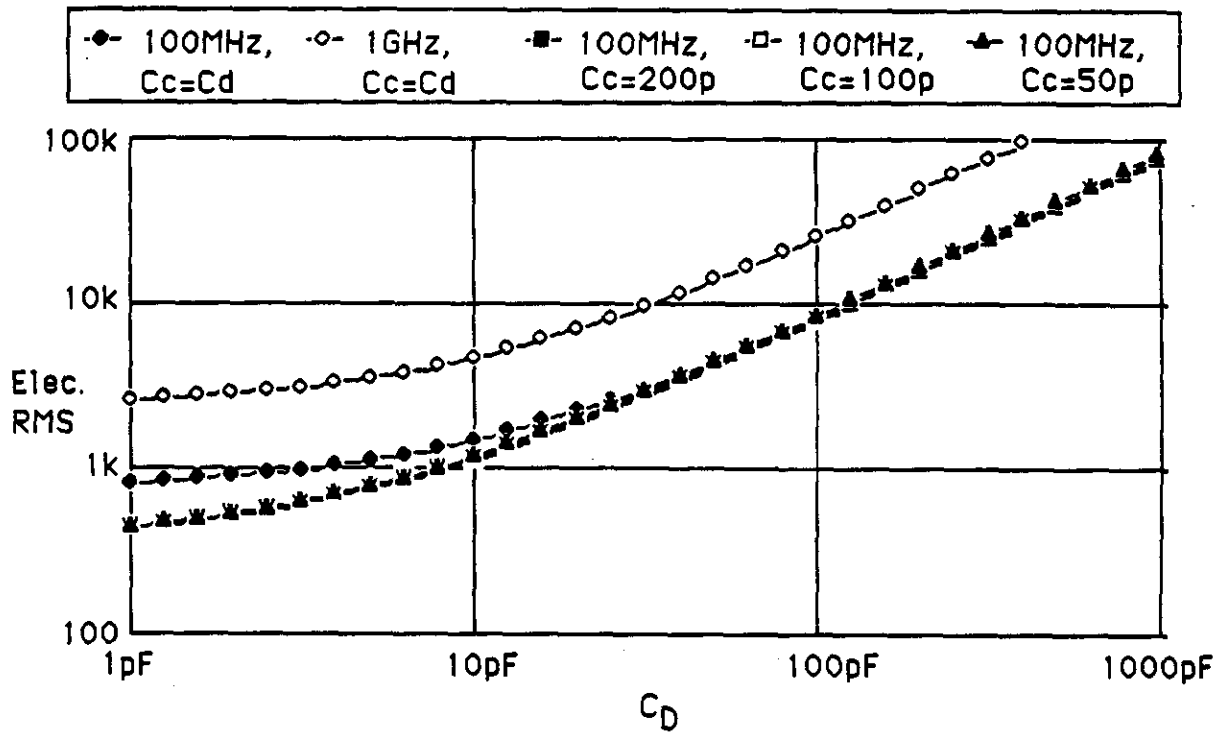


Fig. 4 Input referred noise versus detector capacitance.

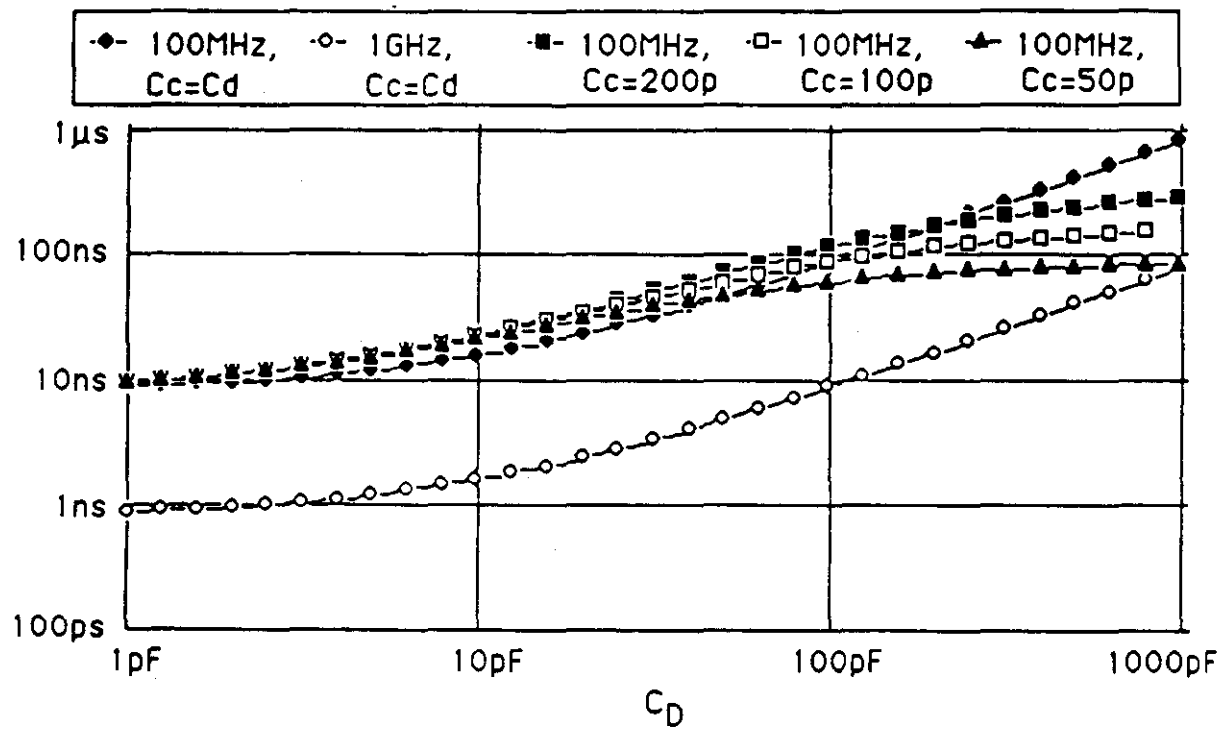


Fig. 5 Output risetime versus detector capacitance.

The electronic specifications of this design are given in Table I. Due to the very small amount of primary ionization produced in warm liquid media (roughly 2000 electron-ion pairs per mm for a minimum ionizing particle), the sensitivity of the design was chosen such that a minimum ionizing particle passing through the cell will generate 1 mV at the amplifier's output, a voltage level which can easily be handled by most commercial readout systems. Based on this technology's current market cost, we estimate that the cost per channel to fabricate this device in large quantities is less than \$40 per channel, a considerable savings over what is commercially available today⁷⁾.

Results of these simulations have already been published⁶⁾ and we reproduce these curves in Figures 3-5. The main point of these simulations is the dependence of output voltage, risetime, and noise on source (i.e., detector) capacitance. In the 10-100 pF range these performance characteristics are not seriously affected. However, these same characteristics rapidly degrade once this capacitance begins to exceed a few hundred pF.

III Test Results

The optimized circuit of Figure 2 was submitted to a BiFET IC manufacturer for monolithic implementation. Although a 1 GHz open-loop bandwidth is the final design goal of this device, the actual speed which we were in fact able to achieve with our first prototype was roughly 10 times slower. These specifications are typical for a standard BiFET IC process. The speed, or f_T value, of the amplifier is determined by the ratio of the JFET transconductance G_M to its own internal capacitance C_{in} by:

$$f_T = \frac{G_M}{2\pi C_{in}}$$

For the prototype made for us, the JFET device specifications were 9 ma/V transconductance and with 20 pF internal capacitance. For a custom (1 GHz) run, we will have to specify a transconductance of 20 ma/V and 4 pF JFET capacitance. (Radiation-hard bipolar technologies in the 20 Mrad range, for instance, are available from Harris Semiconductor Corporation with similar or better JFET device specifications. The radiation hardening here is actually for neutron induced radioactivity, as compared to gamma ray sources.)

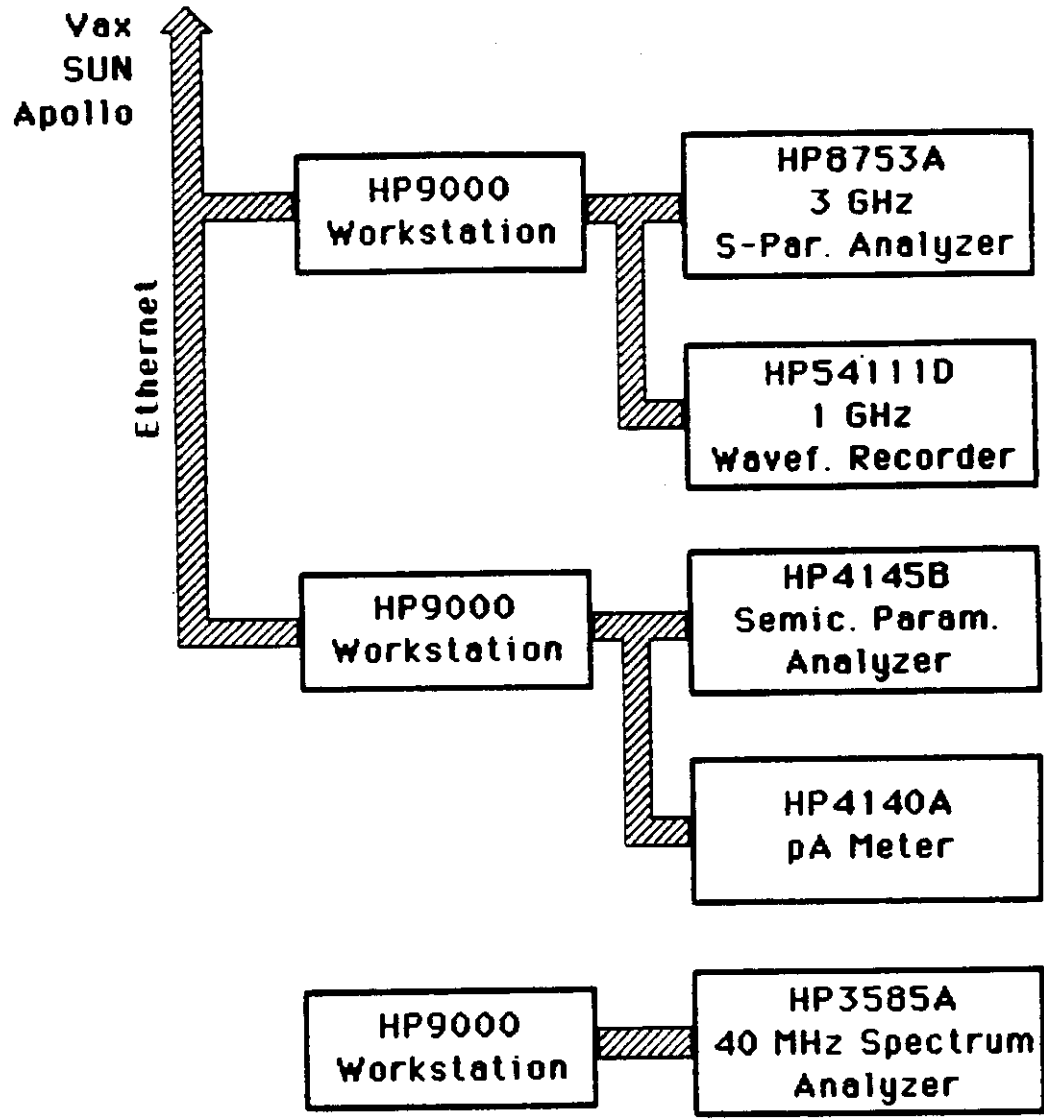


Fig. 6 Measurement configuration in the Texas A&M University VLSI System Evaluation Laboratory.

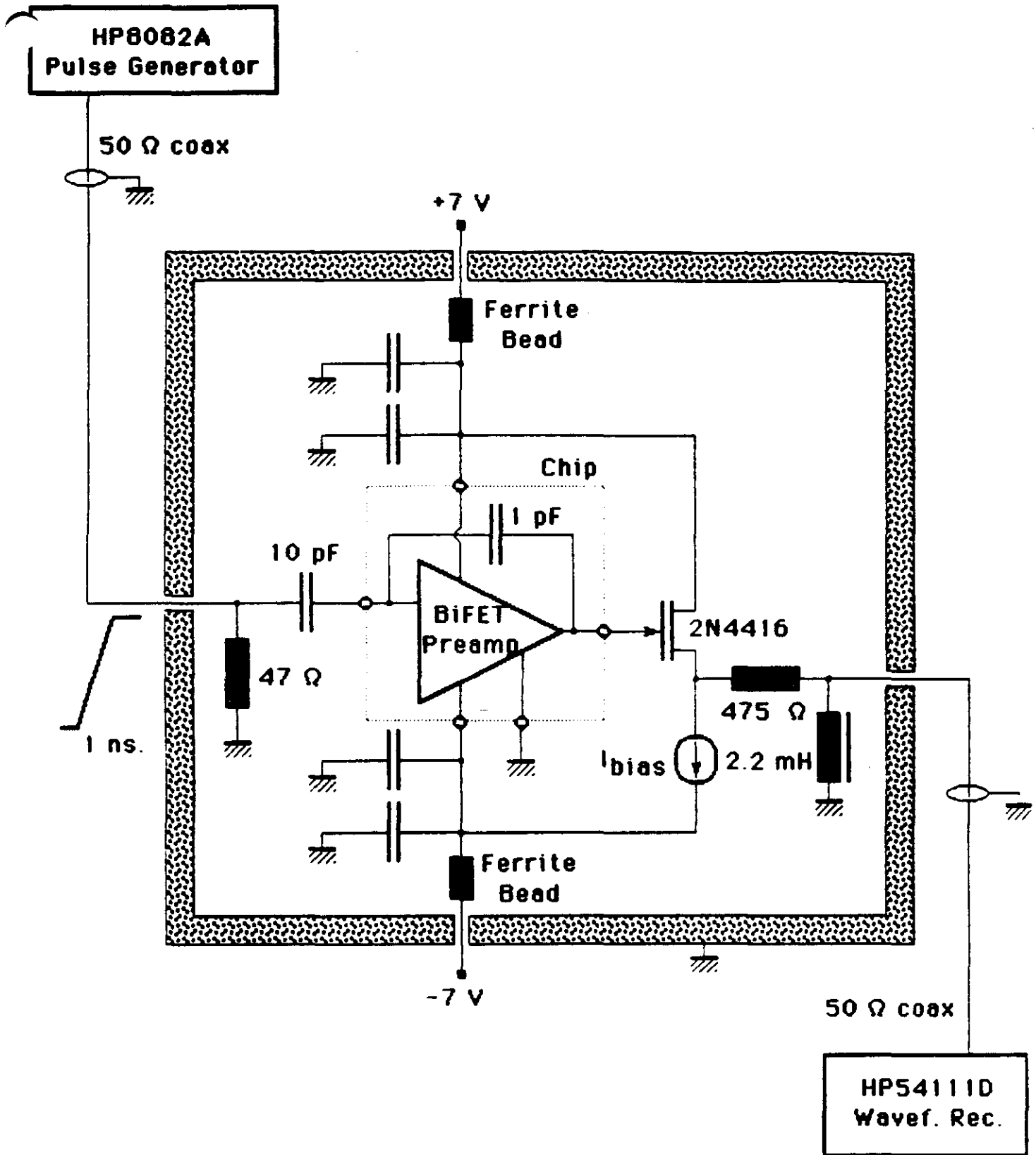


Fig. 7 Actual test setup for testing the prototype charge preamplifier.

The test setup for characterizing the charge preamplifier is shown in Figure 6. The main analytic tool is a 1 GHz digital waveform recorder, model HP54111D. Data taken with this device can be stored and downloaded to a separate workstation for fast Fourier analysis and signal processing. Additional equipment available in the laboratory are semiconductor parameter analyzers, spectrum analyzers, and a picoampere meter, all linked to the same analysis network.

The actual measurement configuration of the charge preamplifier is shown in Figure 7. A relatively low voltage power supply of ± 7 V is necessary to drive this device, for a total power dissipation of 60 mwatts. With a 1 pF internal feedback capacitor and simulated 10 pF source capacitance, the closed-loop gain for this configuration was 10. To reduce low frequency noise, an RL high pass filter was placed at the output of the preamp with a 40 kHz cutoff frequency. An HP8082A pulse generator provided a fast (1 nsec) square wave input to the preamp, which was then readout by the HP54111D digital oscilloscope.

The digitally reconstructed input is shown in Figure 8, along with the charge preamplifier's response in Figure 9. In Figures 10 and 11 we show a time expanded view of the leading and trailing edges in a scale of 20 nsec per division. A risetime of 37 nsec is visible in Figure 10, very close to the f_T value design simulation based on the device specifications provided to us by TI. The corresponding falltime is shown in Figure 11 in the same time scale. The measured 61 nsec falltime is somewhat longer than the 37 nsec risetime, due to the corresponding change in effective transconductance in the JFET with large negative input voltage steps.

The offline fast Fourier transform of these pulses is shown in Figure 12, where the rms noise voltage, V_{rms} , is plotted as a function of frequency. As can be seen in this figure, the spectral noise density characteristic of the charge preamplifier is flat out to 0.5 GHz with a baseline noise level of 5 nV/ $\sqrt{\text{Hz}}$ (-165 dB). The integrated input referred noise over this frequency interval is 100 μV , corresponding to 625 e^- rms for a source capacitance of 10 pF. Included in this noise figure is the contribution from the measurement setup itself, typically 1-1.5 nV/ $\sqrt{\text{Hz}}$. The intrinsic noise of the preamp is therefore less than 500 electrons rms.

INPUT

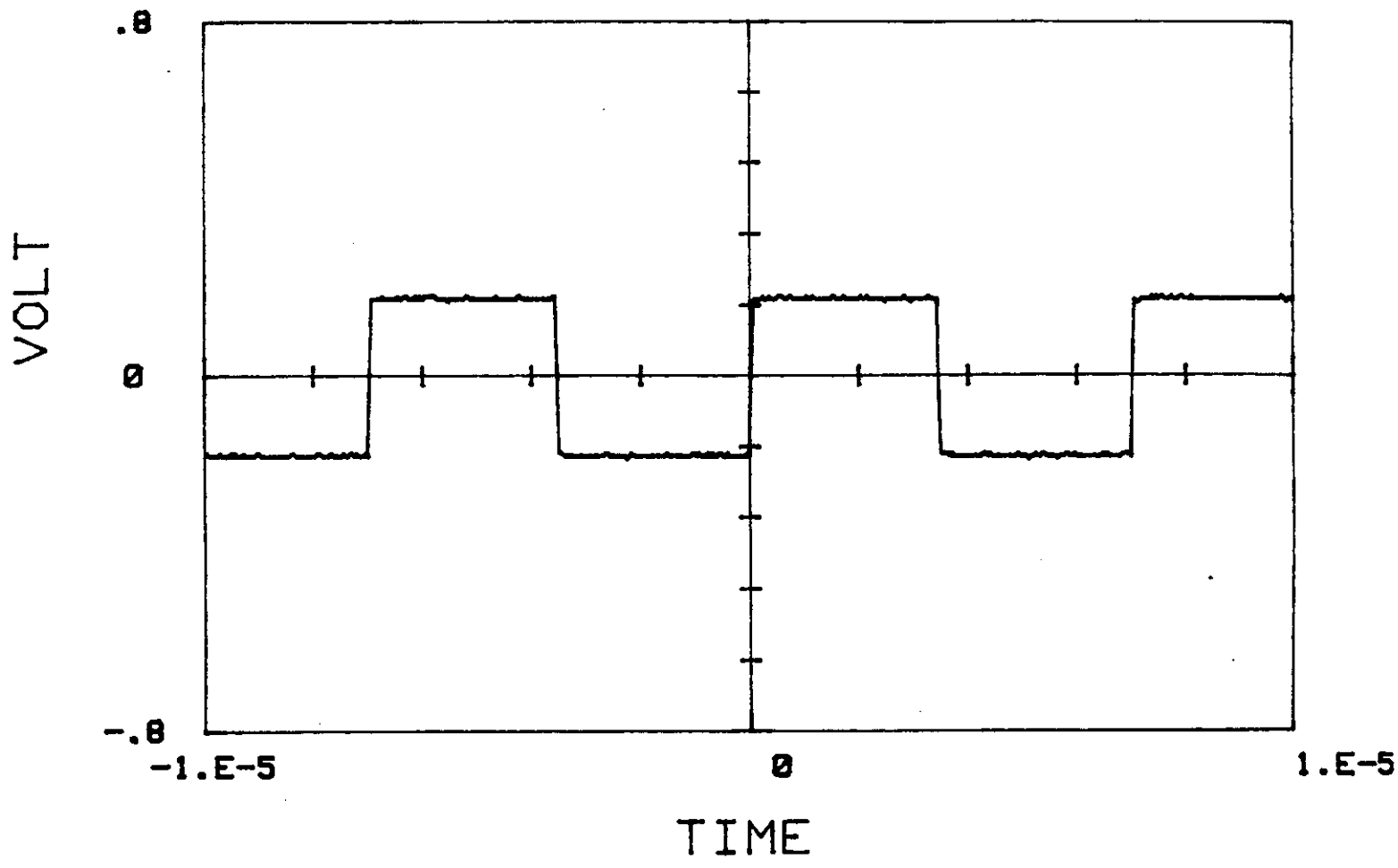


Fig. 8 Digital oscillograph of input square wave pulse.

NEW3_G7_TIME

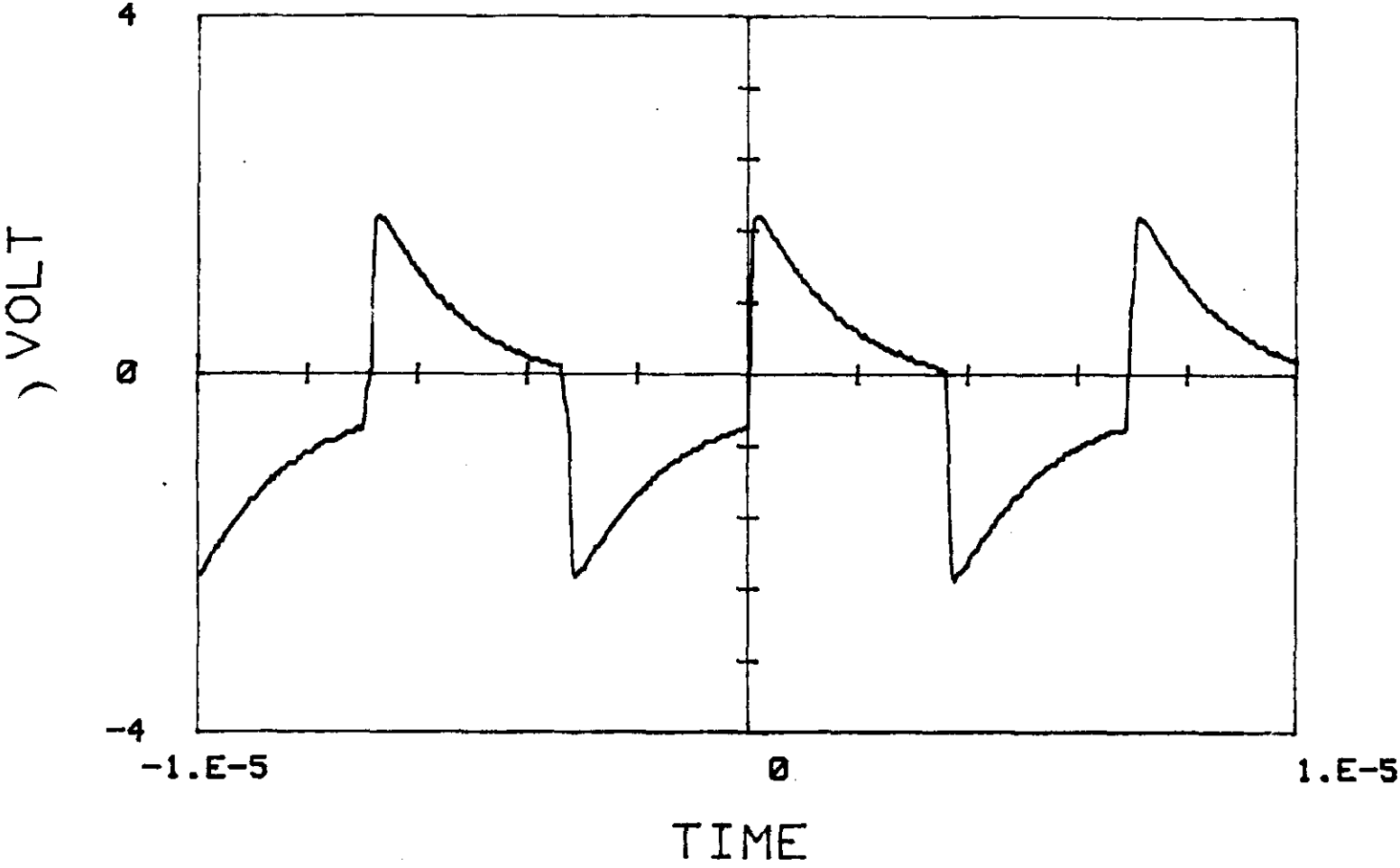


Fig. 9 Digital oscillograph of preamplifier output response with filter.

NEW3_G7_RISE

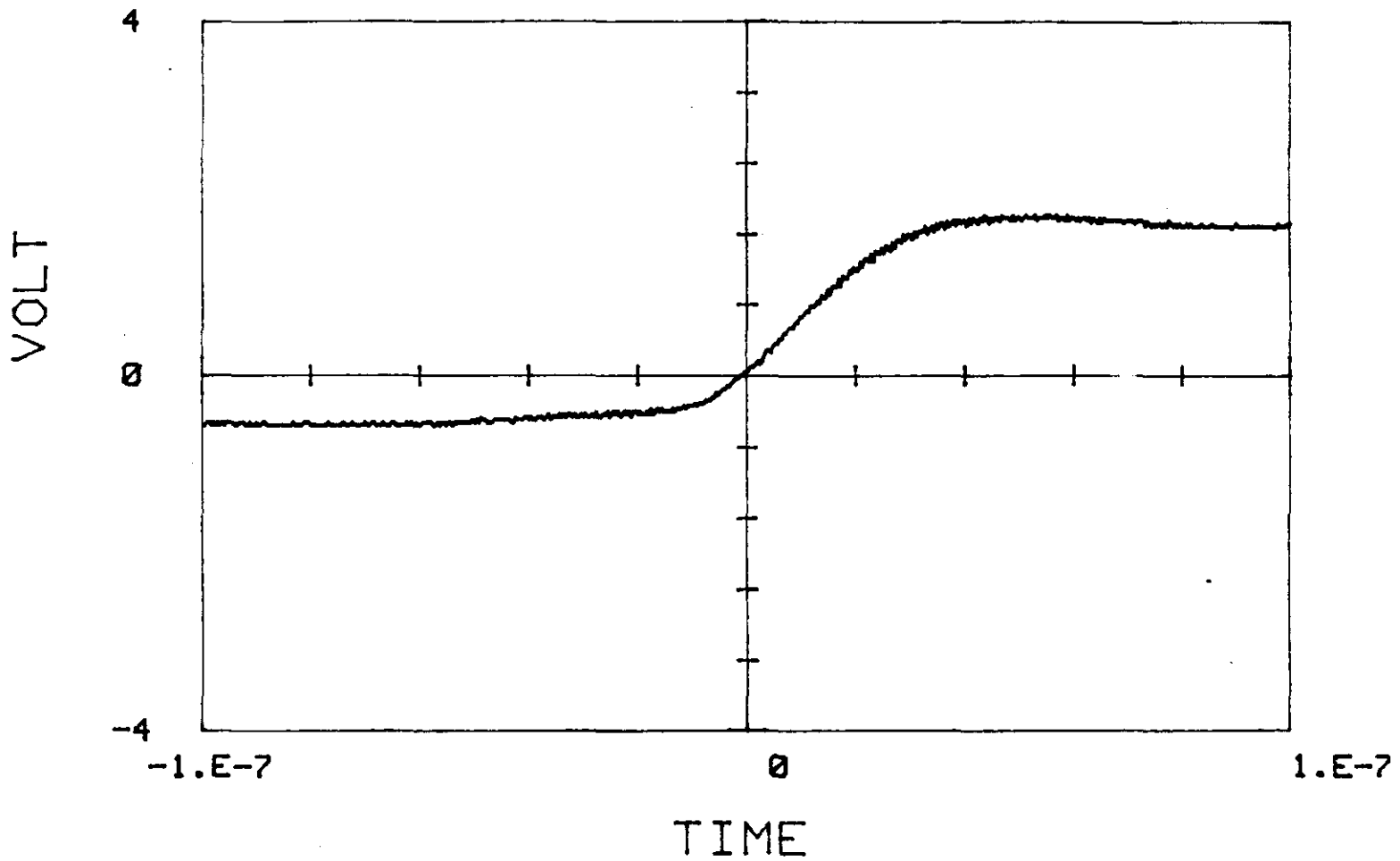


Fig. 10 Leading edge: same as in Fig. 9, but with 20 nsec per division.

NEW3_G7_FALL

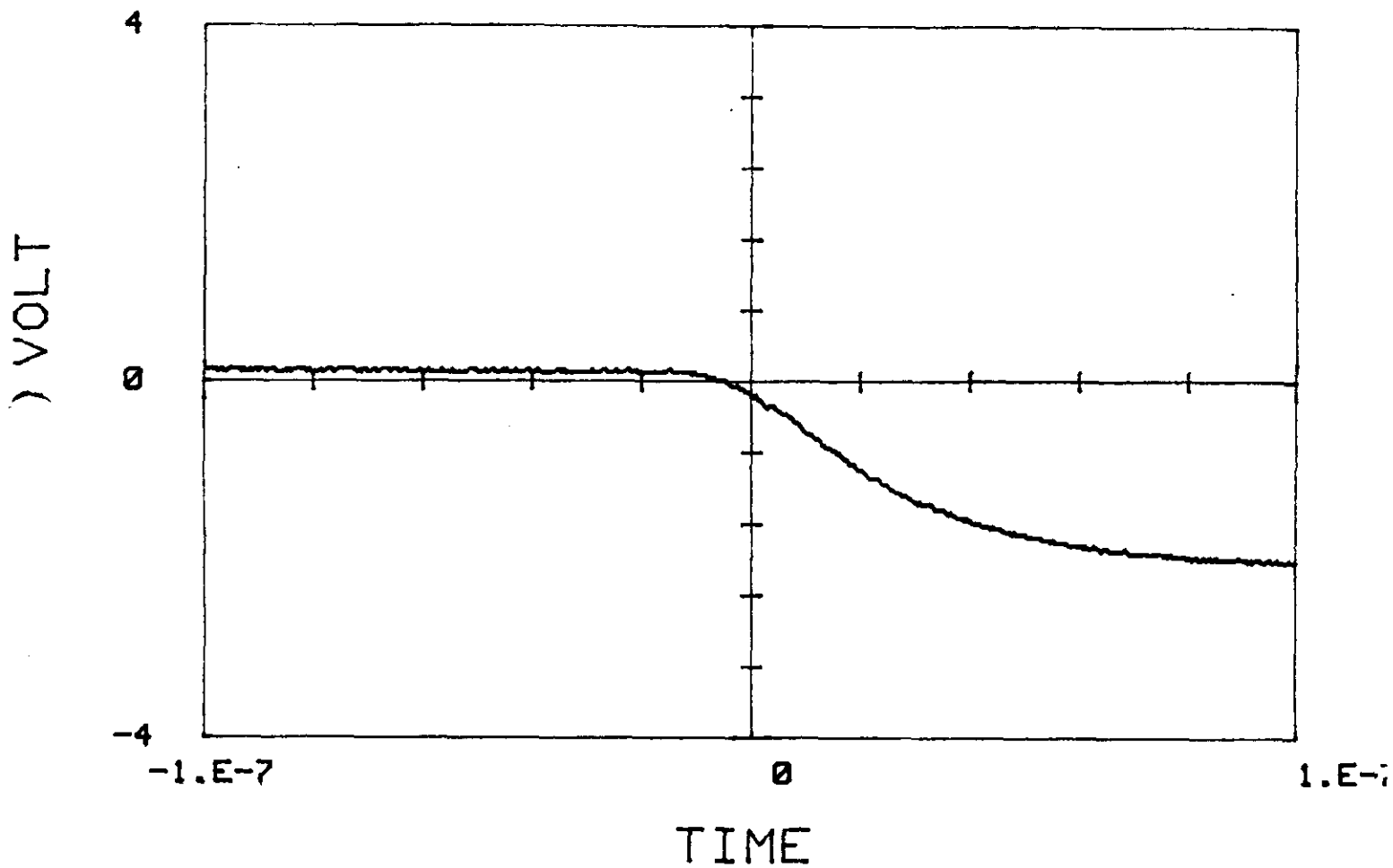


Fig. 11 Trailing edge: same as in Fig. 9, but with 20 nsec per division.

Vrms_NEW

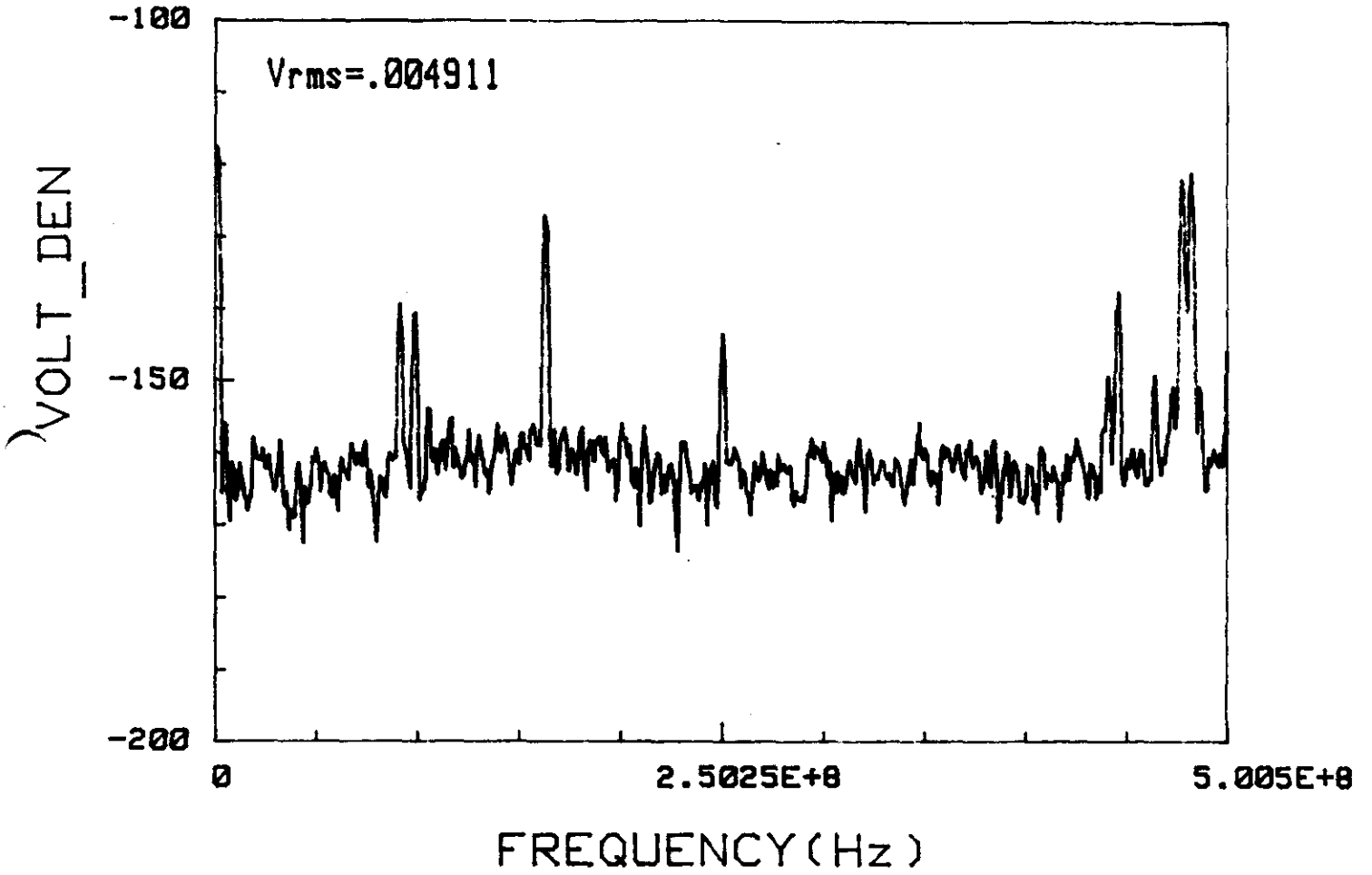


Fig. 12 Spectral noise density (dB). Baseline level is 5 nV/ $\sqrt{\text{Hz}}$.

The extreme sensitivity of this measurement setup is clear from the presence of known peaks in the spectral noise density, most notably from two local FM stations (90.9 and 98.3 MHz), the nearby television monitor, the HP54111D itself, and a local television station (KBTX). This extraneous noise pickup is coming through exposed connecting leads in the measurement setup of Figure 7.

IV Conclusions

We have presented results on the design and operation of a fast, radiation-hard charge preamplifier for calorimetry at the SSC. With a monolithic bipolar technology, we have achieved a 37 nsec risetime device with less than 600 electrons rms noise up to 0.5 GHz. The low power consumption (60 mwatt) and cheap price (\leq \$40 per channel) make this device a very attractive alternative as a fast, radiation-hard, ultra-sensitive front-end charge preamplifier, either for warm liquid calorimetry, or possibly as an amplifier for low gain tetrodes.

V Acknowledgements

We wish to thank many individuals in the U.S. microelectronics industry in supporting us with data and samples of low-noise BiFET IC technology. This work is supported by the U.S. Department of Energy under contract number DE-AS05-81ER40039, HEP and SSC divisions, the Texas Advanced Technology Program, and the National Science Foundation (P.V.). D. DiBitonto wishes to thank the DOE for special support through the Outstanding Junior Investigator Award program.

References

1. D. DiBitonto, et al., "Integrated Ceramic Electrode for Warm Liquid Calorimetry," Proceedings of the Workshop on Calorimetry for the SSC, Tuscaloosa, Alabama, March 13-17, 1989.
2. D. Groom, "Radiation Levels in SSC Calorimetry," Proceedings of the Workshop on Calorimetry for the SSC, Tuscaloosa, Alabama, March 13-17, 1989;
D. Groom, "Radiation Levels in the SSC Interaction Regions," SSC-SR-1033, June 10, 1988.
3. V. Radeka, "Electronics Considerations for SSC Calorimetry," Proceedings of the Workshop on Calorimetry for the SSC, Tuscaloosa, Alabama, March 13-17, 1989.
4. Bipolar DI process technology (dielectrically insulated) is presently available from Texas Instruments with an intrinsic radiation hardness of 1 Grad.
5. At high electric fields, the free electron mobility in tetramethylgermanium (TMGe) is greater than $100 \text{ cm}^2/\text{Vsec}$ (see W.F. Schmidt, Can. J. Chem **55** (1977) 2197).
6. D. DiBitonto, et al., "Advanced Forward Calorimetry for the SSC and TeVatron Collider," Proceedings of the International Conference on Advanced Technology and Particle Physics, Como, Italy, June 13-17, 1988, to be published in Nucl. Instr. and Meth. in Phys. Research **C317**.
7. The Amptek model A-250 charge preamplifier presently retails for over \$400.

Table I

Electronic Target Specifications

Sensitivity	$1\text{V/pC} = .64\text{ mV}/4000\text{ e}^-$
Noise	$500\text{ e}^- \text{ rms}$
Risetime	$2 - 20\text{ nsec}$
Bandwidth	$.1 - 1\text{ GHz}$
Power Dissipation	60 mW per channel
Linearity	$\leq .1\%$
Variation over Temp. and Supply Range	$\leq .5\%$
Technology	Bipolar
Radiation Hardening	$\geq 5 - 20\text{ Mrad}$
Cost	$\leq \$40\text{ per channel}$

Integrated Ceramic Electrode for Warm Liquid Calorimetry

D. DiBitonto, Y. Pang, M. Timko, and S. Sledge

Texas A&M University
College Station, Texas

J. Bobier, J. Ortner, and S. Thome

Hutchinson Technologies, Inc.
Hutchinson, Minnesota

S. Corey and W. Flock

Coors Ceramics
Golden, Colorado

Abstract

We describe the design and construction of a warm liquid media ionization cell to instrument the very forward collider region of the Superconducting Super Collider. This structure consists of an integrated ceramic electrode which combines the functions of mechanical support, anode charge collection, and high voltage feedthrough all into one unit. High internal electric fields and corresponding fast electron drift velocities are in principle achievable through flat, uniform metalization onto a pure ceramic substrate. A procedure to control electron affinic surface contamination below the parts-per-billion (ppb) level is described using an ultra-sensitive mass spectrometer.

Workshop on Calorimetry for the Superconducting Super Collider
Tuscaloosa, Alabama, March 13-17, 1989

I Introduction

In a previous paper¹⁾ we described the design of a small angle calorimeter to instrument the very forward region in present and future hadron (and possibly e^+e^-) colliders. In addition to the potentially rich physics which can be done with such a device, where a large rapidity coverage can be achieved with a relatively compact design, the present forward collider region provides a unique *in situ* testing grounds for new technologies which may be typical even at 90° in an actual SSC operating environment²⁾.

Ionizing detection media based on warm liquid hydrocarbons such as 2,2,4,4 tetramethylpentane (TMP), tetramethylsilane (TMS), or even tetramethylgermanium (TMGe) are now considered to be serious candidate media due to their high intrinsic radiation hardness and speed. Calorimetry configured with a 4:1 (lead) radiator to liquid media ratio can be made compensating³⁾, whereby the electromagnetic and hadronic energy responses are equalized. By comparison, compensation with liquid argon calorimetry is not possible. Although chemical decomposition of warm liquids after exposure to radiation is unavoidable⁴⁾, passive compounds produced such as hydrogen and methane (both non-electron affinic) can be collected and vented internally without loss of detector sensitivity.

Conventional electrode designs using pre-stressed metal shim stock as in the UA1 U TMP calorimeter design are limited in their ability to maintain high electric fields⁵⁾. Edge effects near the electrode periphery have been responsible for recent low voltage operating conditions typically 400-1000 V across a 1.25 mm gap which, for TMP, results in a corresponding electron drift time across the gap of more than 700 nsec. We propose an alternative anode structure based on a smooth, uniformly metalized ceramic plate with superior high voltage standoff properties. Prototype electrodes have already been manufactured with local a surface roughness of less than $2 \mu\text{m}$.

As in the case of photomultiplier tubes, which exhibit a hypersensitivity to contamination present in their internal vacuum, warm liquids and their containers must also operate under very strict purity control whereby electron affinic contaminants such as chlorine are kept below the ppb level. We describe a procedure which is capable of achieving these purity levels with a quantifiable technique based on residual gas analysis.

II Ceramic Electrode

An exploded view of the warm liquid cell is shown in Figure 1, along with its mechanical, electrical, and material specifications in Table I. This device is essentially a four-piece unit, consisting of an integrated ceramic electrode, an outer metal band wall, and two outer metal "skins" 0.5 mm thick. The cell has two drift gaps on both sides of the (double sided) metalized electrode, for a total thickness of 6 mm. Filling ports at 45° from both wall sides provide internal access for ultra-high vacuum cleaning and filling.

In the present application of a small angle calorimeter upgrade for the CDF experiment at the Fermilab TeVatron Collider, or possibly as a two-photon tag at LEP, this cell has been designed to fit just above the beam pipe. In this rapidity interval, the anode pad size covers 1 rapidity unit and $\Delta\phi$ of 45° , which are matched to the transverse hadronic shower development expected in this region. Segmentation into smaller units may not be necessary, although it is certainly not limited with this technique.

The anode patterns are created with a thick film processing technology which fuses a molybdenum-manganese alloy onto a pure alumina plate, much like an ordinary printed circuit board is manufactured. The main advantage of this approach is that any anode pattern can be achieved by simply changing the corresponding silk screen outline. Connecting leads are also patterned onto the same silk screen to an external high voltage and signal feedthrough, which is also part of the same ceramic structure. This design completely eliminates the need for separate external high voltage feedthroughs, which would in turn be welded externally to the outer frame and internally to their respective anode plate. A separate dielectric insulator is fired around the feedthrough areas to provide electrical insulation from an ultra-high vacuum seal to the surrounding metallic vessel (see Figure 2). The procedure detailing the production sequence, assembly, and characterization of this electrode and its surrounding vessel is given in the Appendix of this report.

The electrical capacitance per pad is roughly 20 pF which gives this detector its intrinsic high bandwidth and low noise specifications (see ref. 1). For the 2 mm gap in this structure and operating voltage of 6 kV, the maximum drift time in a TMGe medium can be as fast as 75 nsec, where μ_{TMGe} is nearly $100 \text{ cm}^2/\text{Vsec}^6$).

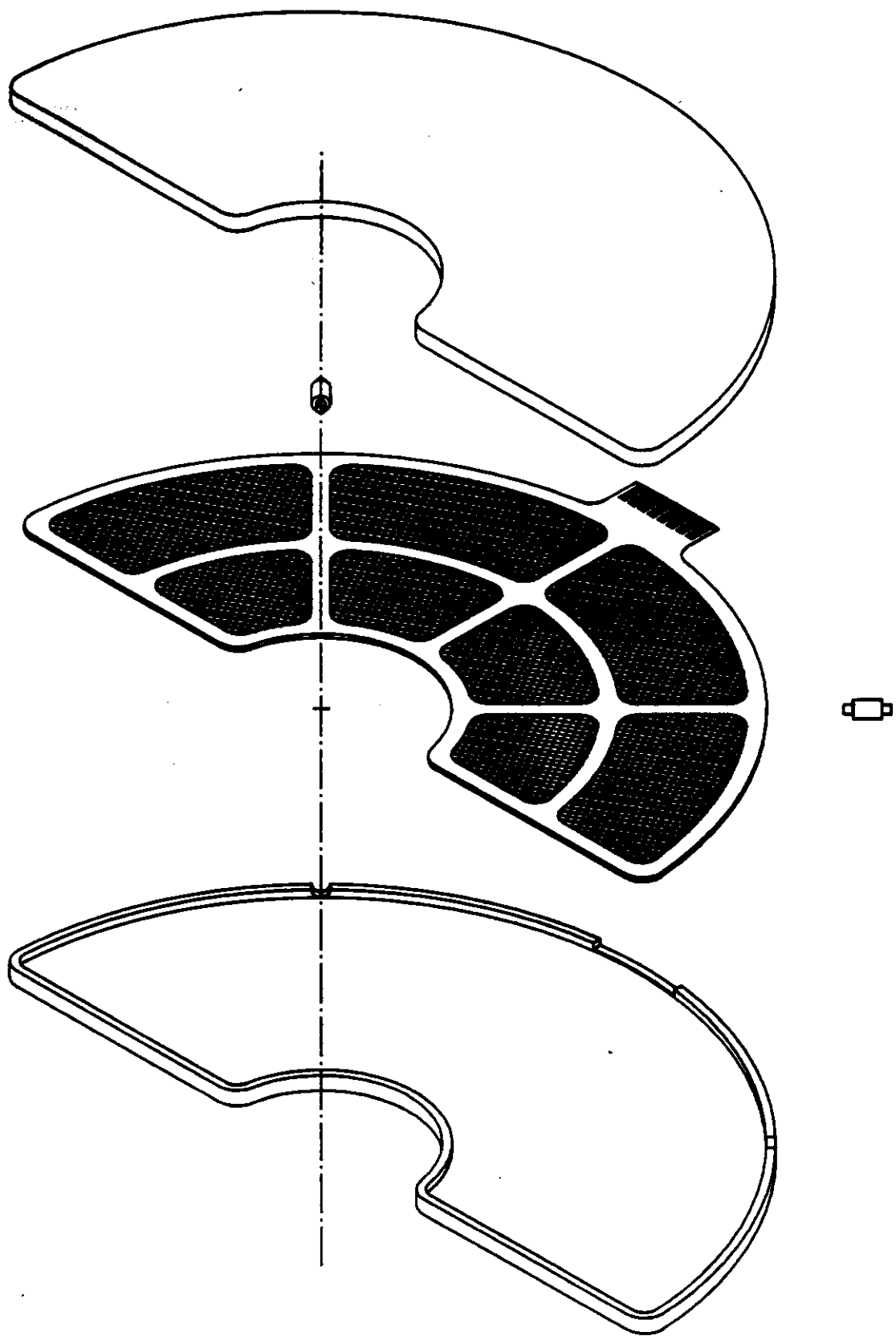


Fig. 1 Exploded view showing metalized ceramic electrode and outer steel vessel.

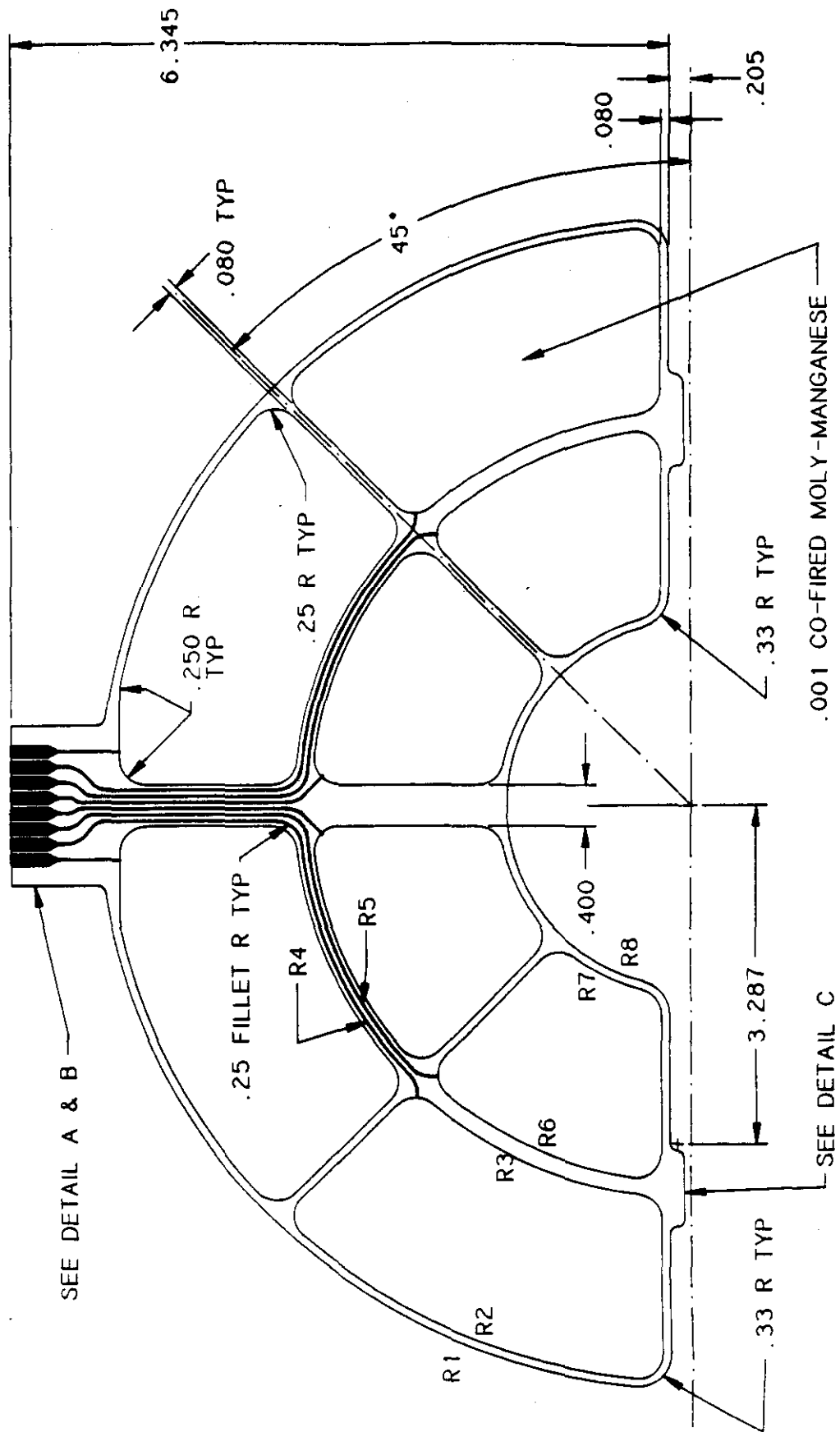


Fig. 2 a) Metalization pattern for anode pads and feedthrough connections.

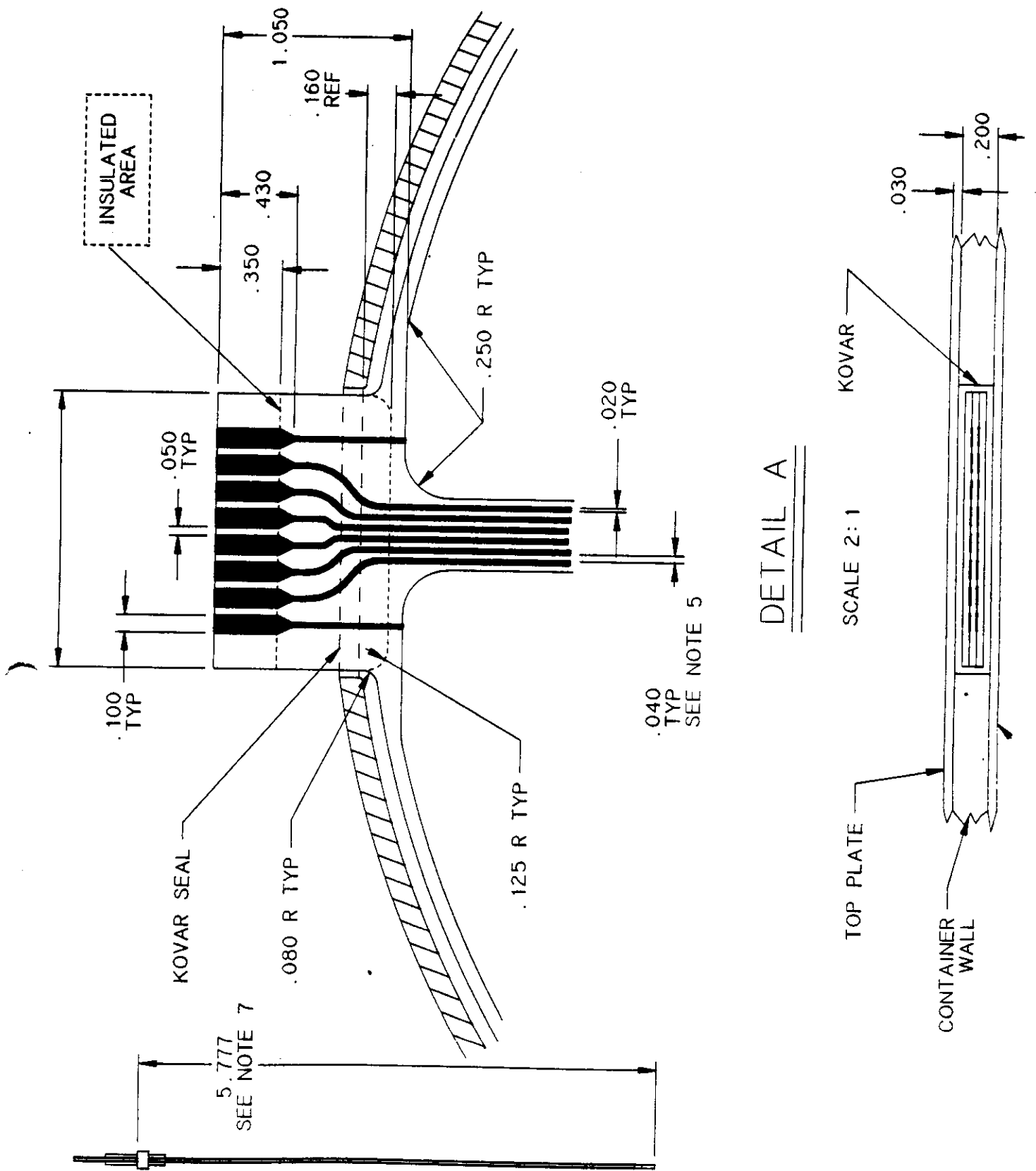


Fig. 2 b) Detail showing insulating dielectric layer, with side and end views.

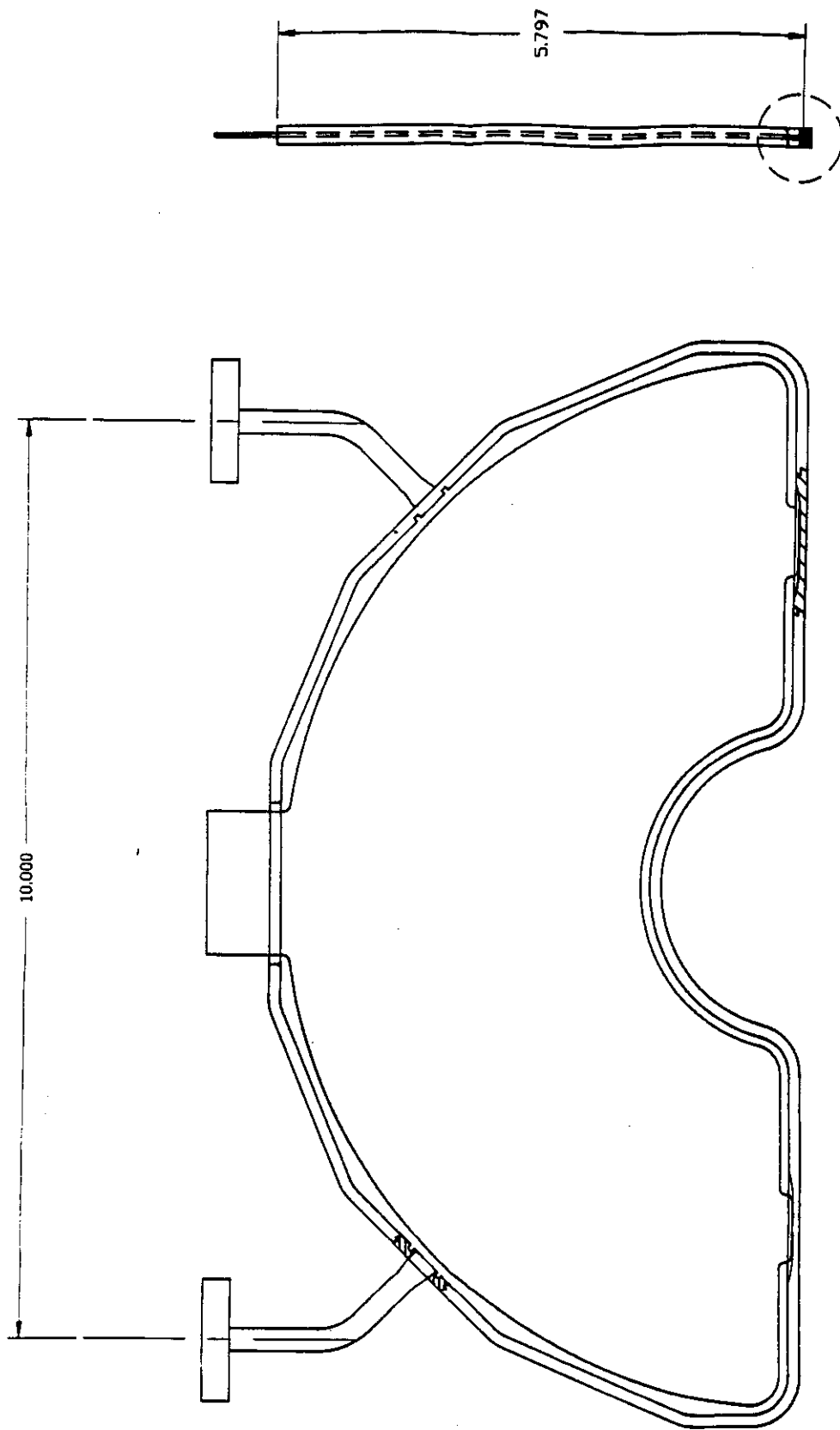


Fig. 2 c) Outer vessel wall with grooved inner slots for electrode support.

III Surface Characterization and Purity

To characterize each ceramic electrode for surface integrity and purity, a small calibration test sample is fired on the same alumina plate which can then be handled more easily with standard material science evaluation procedures. Electron micrographs of one such representative sample are shown in Figure 3 for magnification scales of 1000 μm , 100 μm , and 10 μm .

In Figure 3 a) a side view of this 1 mm thick sample clearly shows the laser scoring used to cut the electrode pattern from its original plate. The brighter surface on the top left side is the MoMn metalized area, typically 25 μm thick. A closeup of the ablated zone cut by laser approximately 300 μm deep is shown in Figure 3 b). Under higher magnification the transition area between the metalization and the ceramic is shown in Figure 3 c), indicating a very smooth, well defined edge with no protruding structures.

In Figure 3 d) we show a 10 μm scale closeup of the very edge of metalization, in which the actual sintered microspheres of MoMn are now visible, typically $\leq 2 \mu\text{m}$ in diameter. Under the intense firing conditions (1600 $^{\circ}\text{C}$), this metal fuses and bonds to the ceramic substrate, leaving no visible sharp edges anywhere on the metalization. The resulting surface and edge are then electrostatically smoother than an actual piece of exposed shim stock that is simply supported by insulating spacers. Additional protection from high voltage breakdown is afforded by the 2 mm ceramic boarder along the metalized edges and between the inner vessel walls (see Figure 2).

A. Preliminary XPS Characterization

To check for gross contamination above the parts-per-thousand level, these samples are characterized by x-ray photoelectron spectroscopy (XPS) with a Kratos XSAM 800 System. In Figure 4 the characteristic emission peaks in the spectrum of photoelectron binding energies are used to identify elements on the surface to a depth of approximately 20 angstroms.

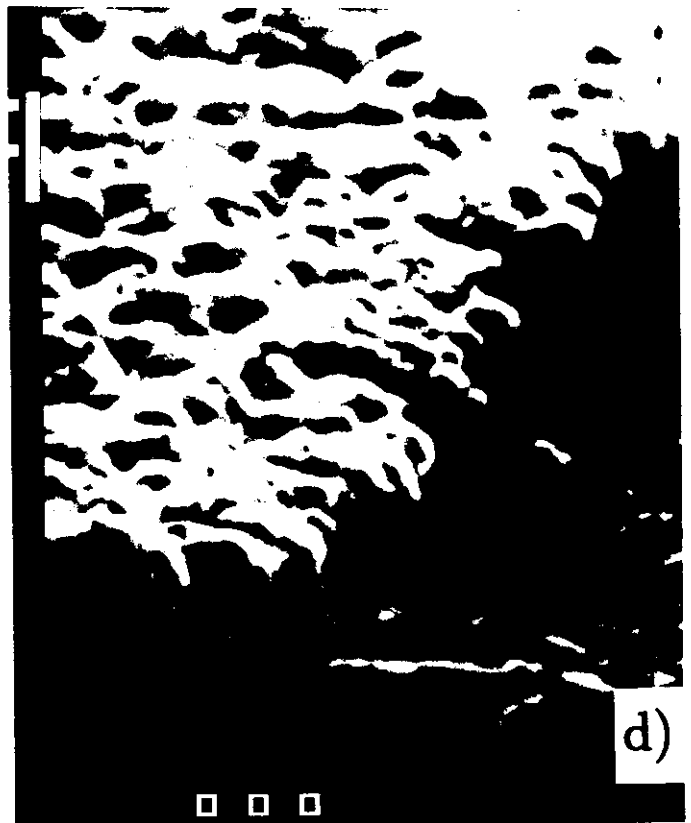
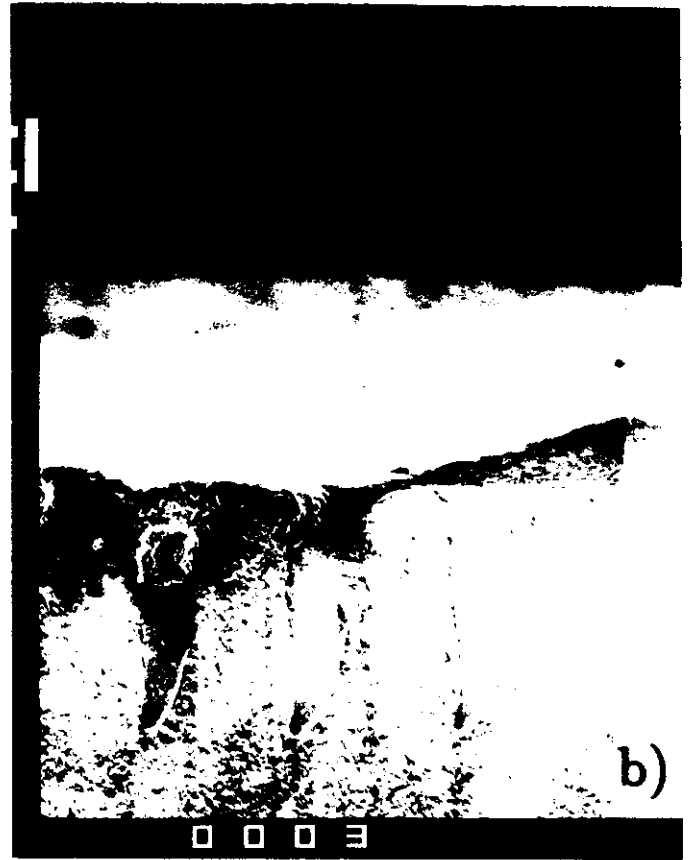


Fig. 3 Ceramic test sample: a) 1000 μm ; b), c) 100 μm ; d) 10 μm .

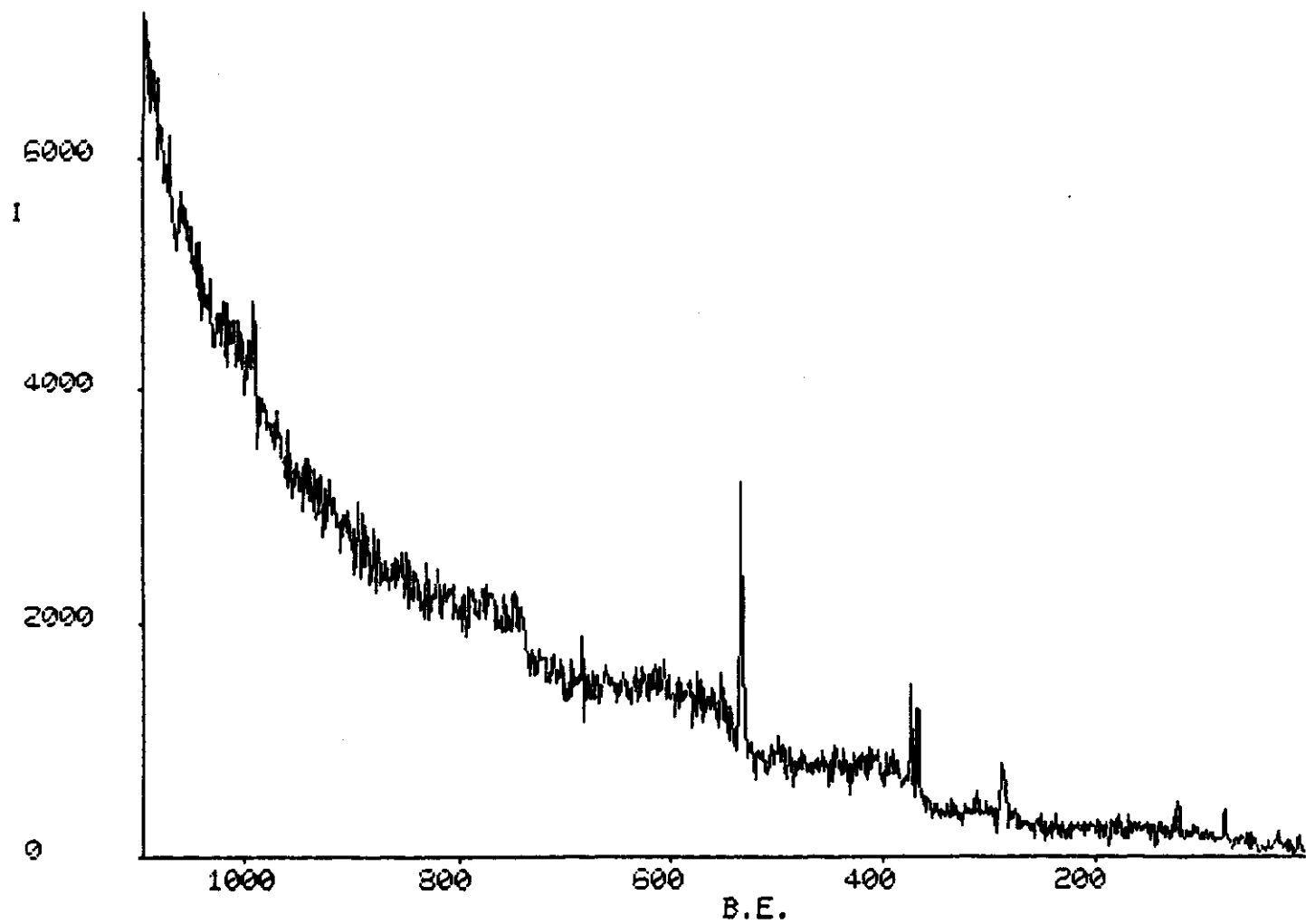


Fig. 4 XPS spectrum of ceramic test sample.

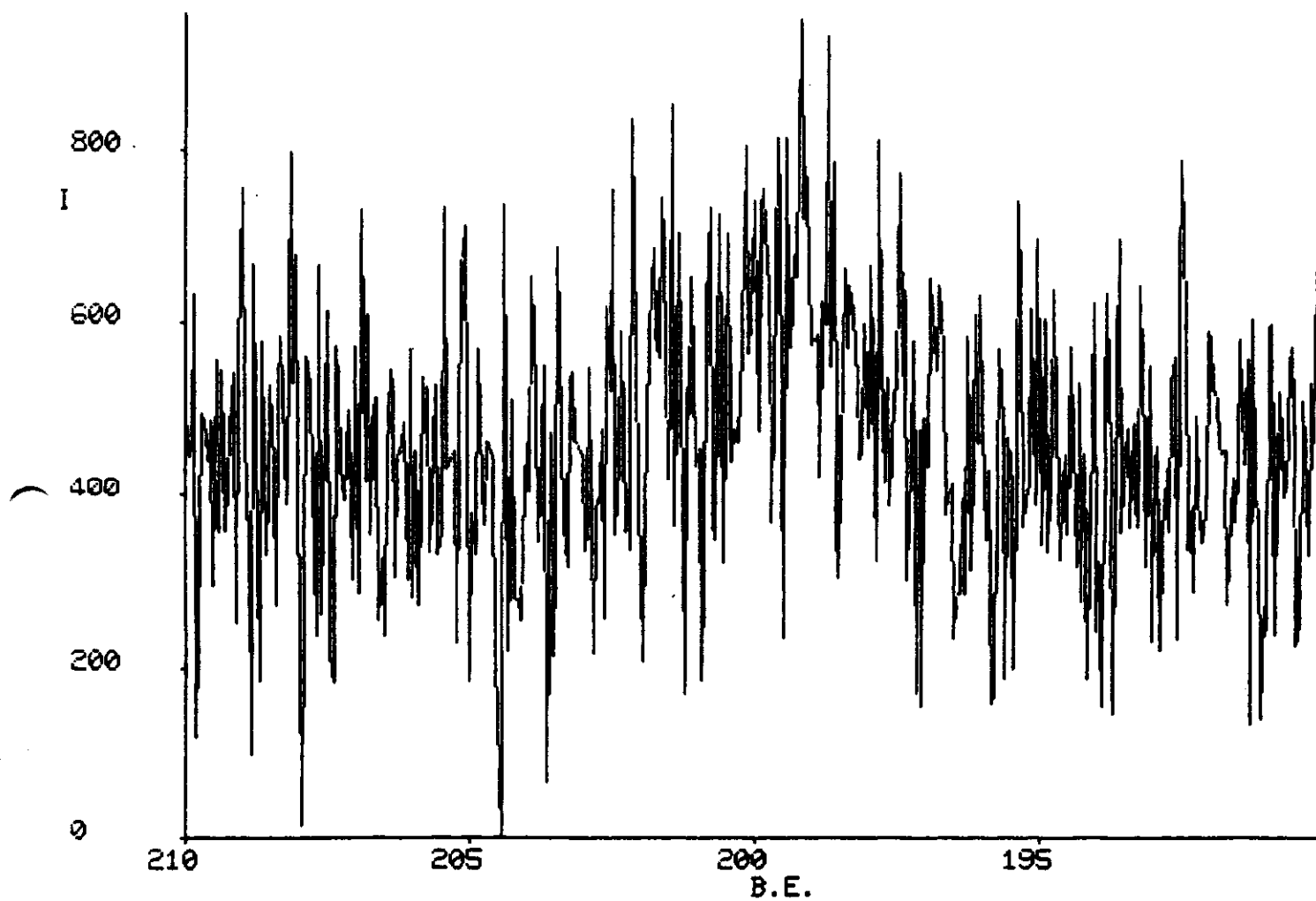


Fig. 5 a) XPS spectrum in chlorine interval before heat treatment.

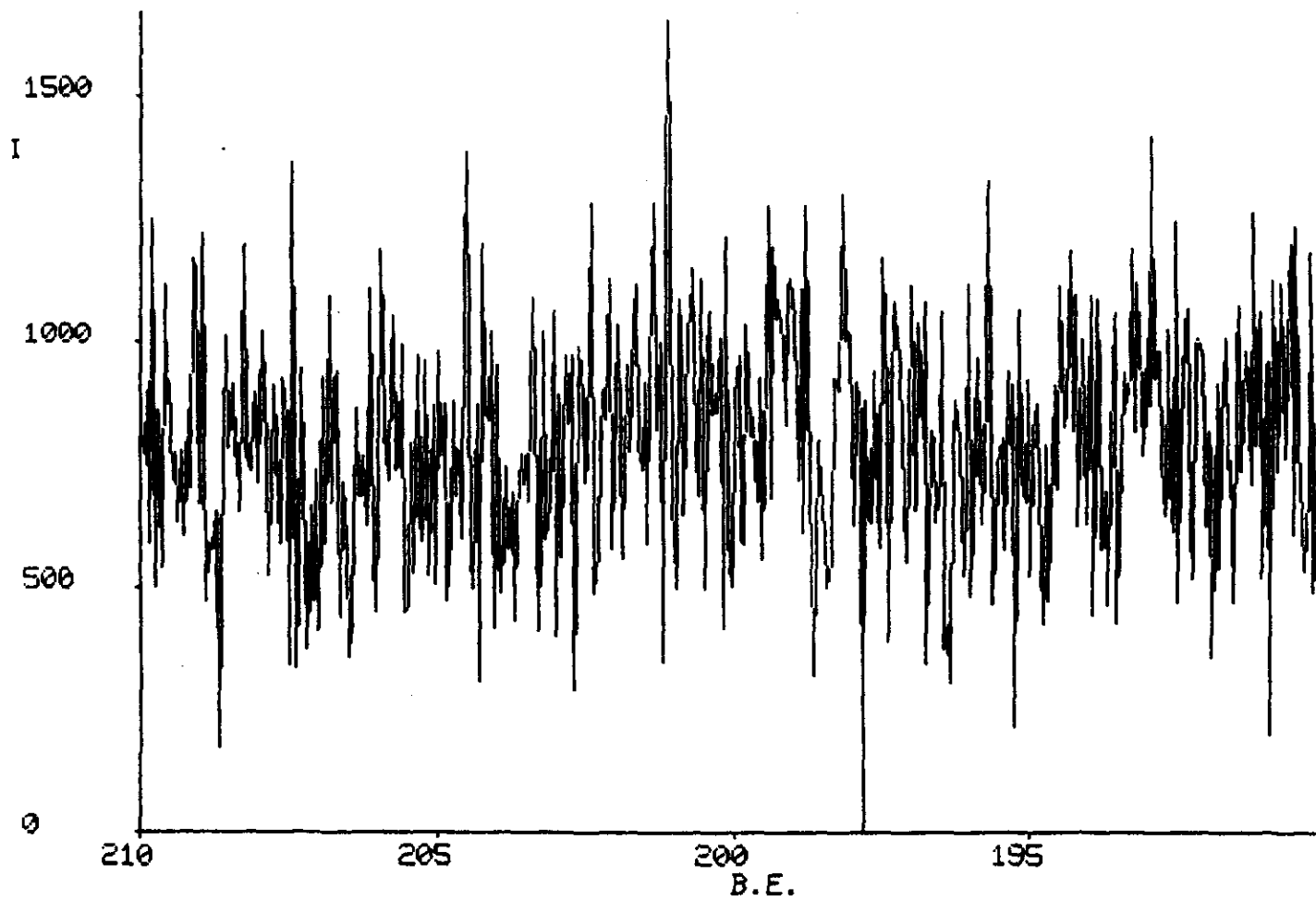


Fig. 5 b) Same as in Fig. 5 a), but after heat treatment.

In an earlier related test of chlorine sensitivity, a sample piece of kovar was electroplated with nickel in a chemically active bath containing HCl. (A 2-3 μm layer of nickel must first be applied to both the kovar and otherwise inert MoMn surface in order to braze the kovar ring in Figure 2 a.) The resulting XPS spectrum for this kovar sample is shown in Figure 5 a), in which a clear emission peak near 200 eV is evident, characteristic of the presence of chlorine. It is noteworthy to mention that even after this sample was cleaned by argon glow discharge, which removed roughly 100 angstroms of surface material, the same chlorine peak was still visible, indicating that chlorine was trapped interstitially throughout the nickel during the plating process.

In Figure 5 b) we show the effects of heat treatment to this same sample, which was subjected to a 950 °C bakeout at 10^{-3} Torr. The resulting spectrum is subsequently void of any significant structure in the chlorine interval, indicating that any residual contamination is less than roughly one part-per-thousand. As an alternative to electrochemical plating, Coors Ceramics is now reducing Ni_2O_3 onto the metallic surfaces to deposit the nickel for brazing purposes.

B. Characterization by RGA

For the specific application of a TMP ionizing medium, 1 ppb contamination corresponds to very nearly 1.0×10^{-10} Torr in partial pressure of the same contaminant⁷⁾. By monitoring the partial pressures of specific electron affinic contaminants (such as fluorine, chlorine, CO, and O₂) during an ultra-high vacuum bakeout, the corresponding ppb contamination levels present within the vessel can then be measured.

The heart of this detecting system is an SX-200 quadrupole mass spectrometer (V.G. Instruments, Inc.) with a partial pressure sensitivity of 10^{-14} mbar and an atomic mass to charge range from 1 to 200. The ultra-high vacuum setup which incorporates the RGA system is shown in Figure 6. Following a Balzers turbomolecular pump section with 50 l/sec pumping capacity, a Varian Starcell Vaclon ion pump near the vessel brings the final total pressure down to less than 10^{-9} Torr.

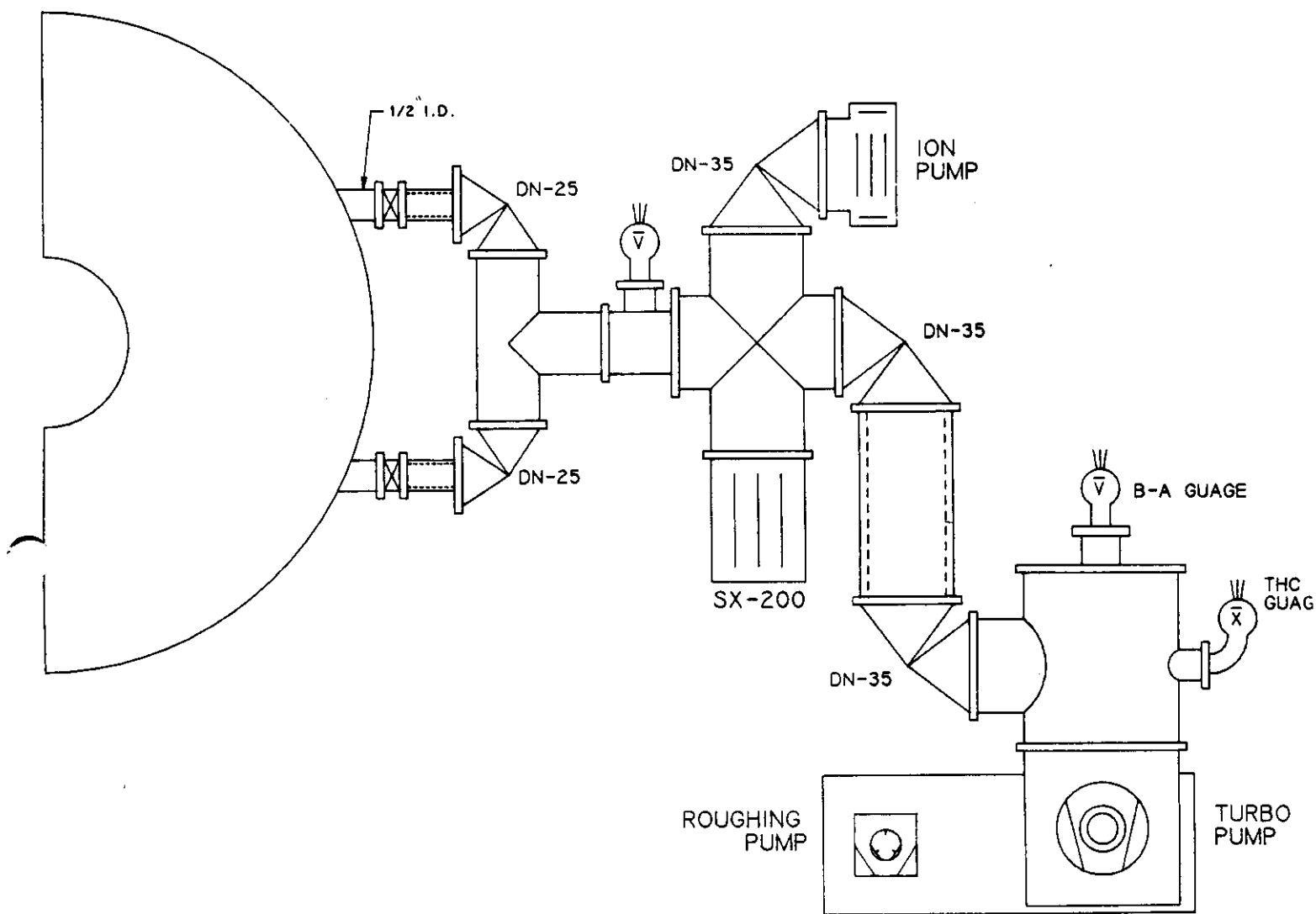
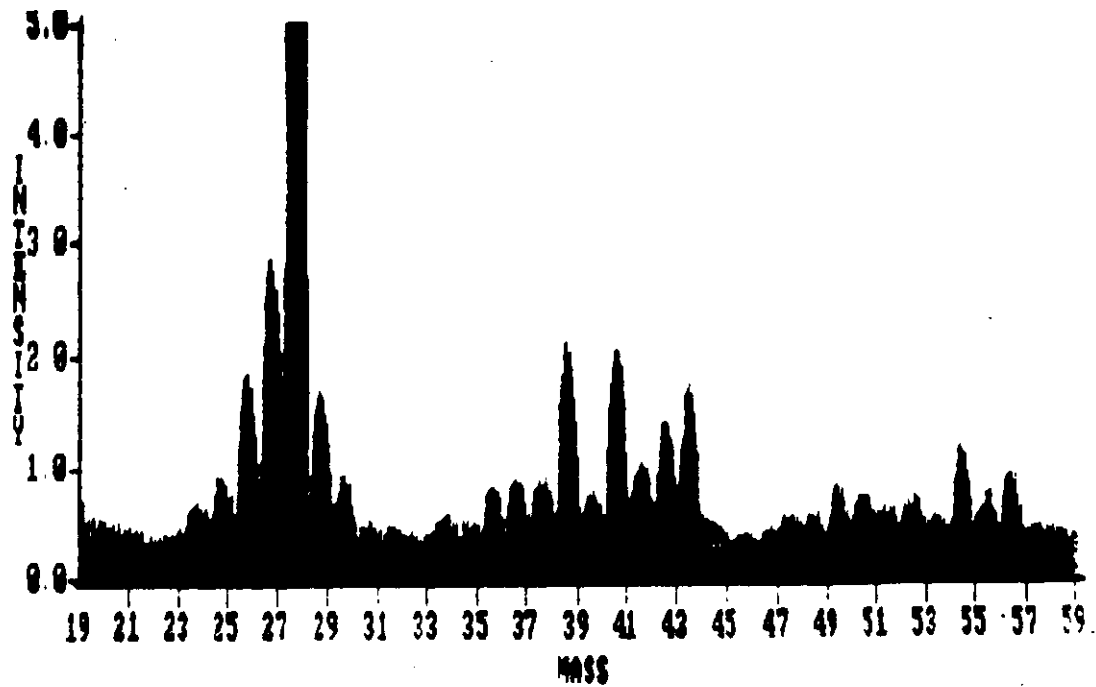
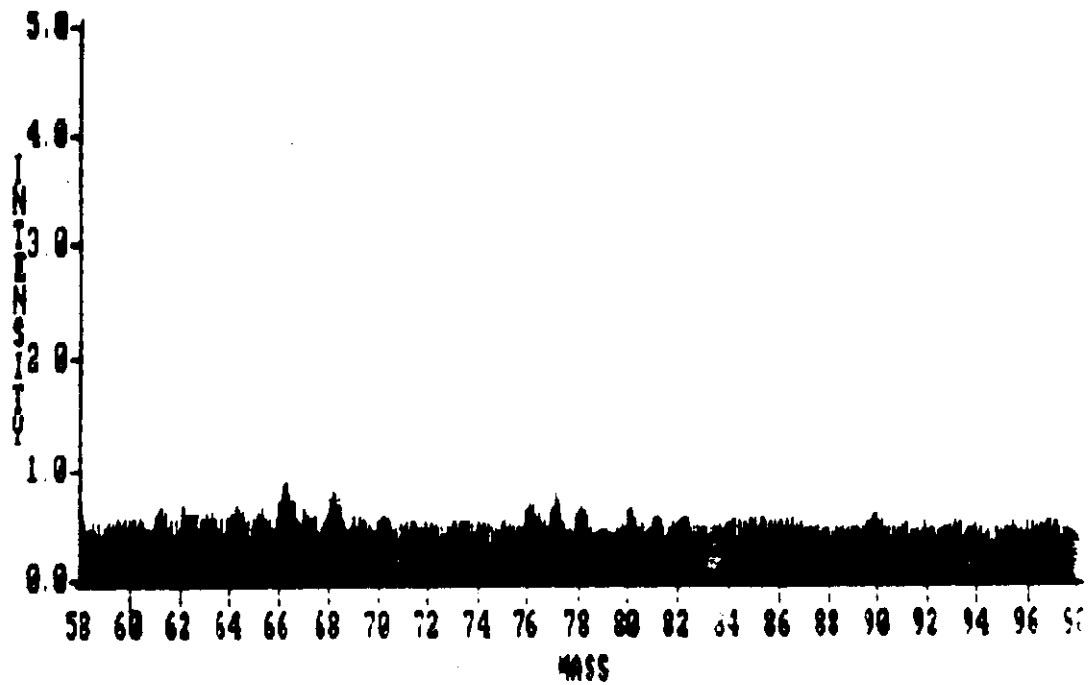


Fig. 6 Setup for ultra-high vacuum and RGA characterization.



RANGE	MAGNIFY	AVERAGE	START	SPAN	STORE	CURSOR
F-10	X 2	64	19	41	OFF	19.13



RANGE	MAGNIFY	AVERAGE	START	SPAN	STORE	CURSOR
F-10	X 2	64	58	41	OFF	58.13

Fig. 7 RGA mass spectrograph at 10^{-10} Torr within prototype vessel.

The actual procedure detailing the assembly and monitoring of the warm liquid vessel with the SX-200 is outlined in the Appendix. This procedure, although complicated, is followed to guarantee that strict purity control is maintained at every step of the assembly. Ultra-high vacuum bakeout and cascade rinses in de-ionized water (17 M Ω cm) are the essential steps in removing surface contamination.

An actual mass spectrum taken with a prototype vessel is shown in Figure 7 for masses above and including fluorine ($m = 19$). The strong peak at 28 is characteristic of N₂, while those near 34, 36, and 43 are characteristic of the known hydrocarbons CH₅OH, CH₆OH, and C₃H₇ (propyl). In the mass interval between 70 and 72, where one would expect to see diatomic chlorine Cl₂, no significant structure is visible above the noise level of 0.5×10^{-10} Torr, indicating a maximum possible chlorine contamination of less than 0.5 ppb.

IV Conclusions

A novel electrode design has been described which integrates the functions of mechanical support, anode charge collection, and high voltage feedthrough all into one unit. The surface smoothness is typically less than 2 μ m with no visible sharp protruding edges anywhere on the metalized surface. The corresponding high voltage standoff properties of this electrode are expected to be far superior to any conventional electrode scheme.

A procedure is described to prepare and characterize surfaces coming in contact with warm liquid media. For a TMP fluid media, the contaminant sensitivity at the ppb level is correlated to a partial pressure detection sensitivity of 10^{-10} Torr. Calibration spectra taken with a prototype vessel indicate that with this procedure the maximum chlorine contamination within the cell is less than 0.5 ppb.

V Acknowledgements

This work is supported by the U.S. Department of Energy under contract number DE-AS05-81ER40039, HEP and SSC divisions, and the Texas Advanced Technology Program. D. DiBitonto wishes to thank the DOE for special support through the Outstanding Junior Investigator Award program.

References

1. D. DiBitonto, et al., "Advanced Forward Calorimetry for the SSC and TeVatron Collider," Proceedings of the International Conference on Advanced Technology and Particle Physics, Como, Italy, June 13-17, 1988, to be published in Nucl. Instr. and Meth. in Phys. Research **C317**.
2. D. Groom, "Radiation Levels in SSC Calorimetry," Proceedings of the Workshop on Calorimetry for the SSC, Tuscaloosa, Alabama, March 13-17, 1989;
D. Groom, "Radiation Levels in the SSC Interaction Regions," SSC-SR-1033, June 10, 1988.
3. R. Wigmans, "The Spaghetti Calorimeter," Proceedings of the Workshop on Calorimetry for the SSC, Tuscaloosa, Alabama, March 13-17, 1989.
4. R. Holroyd, "Effects of Radiation Damage to TMP, TMS, and Liquid Argon Solutions," SSC-SR-1035, p. 335, June, 1988.
5. A. Givernaud, "Status of UA1 Upgrade," Proceedings of the Workshop on Calorimetry for the SSC, Tuscaloosa, Alabama, March 13-17, 1989.
6. W.F. Schmidt, Can. J. Chem **55** (1977) 2197.
7. For TMP, $\rho = 0.72 \text{ g/cm}^3$ with a gram molecular weight of 128.

Table I**Vessel Specifications****Mechanical**

Inner Radius	4 cm
Outer Radius	15 cm
Plate Thickness	0.5 mm
Electrode Gap	2.0 mm
Anode Structure	1.0 mm
Total Thickness	6.0 mm
Rapidity-Phi Coverage per Channel	$\Delta y=1, \Delta\phi=\frac{\pi}{8}$

Electrical

Number of Channels	8 pairs
Mean Channel Capacitance per Pad	18 pF
Operating Voltage	4-6 kV

Materials

Outer Plates and Rim	304 L stainless steel
Anode Pads and Leads	Moly-Manganese (25 μm)
Anode Pad Support	Ceramic (ADS 995)
HV Feed-through	Copper brazed Kovar- Al_2O_3

APPENDIX

PRODUCTION SEQUENCE FOR CERAMIC ELECTRODE

1. Alumina Plate (ADS 995, 0.040 in) fired at 1600 °C
2. Laser Cut Electrode Shape
3. Co-fire Moly-Manganese Anode and Leads at 1350 °C
0.001 in thick, $\leq 60 \text{ m}\Omega/\square$, 50 μin surface rough.
4. Dielectric Insulator (ADS 995) fired at 1450 °C
5. Co-fire Moly-Manganese Strip for Kovar Braze
6. Reduce 0.1 mil Nickel (Ni_2O_3) on Tab and Brazing Surface
7. Electrode Pre-Cleaning (HTI)
(to be determined on basis of RGA analysis)
8. Braze Kovar Collar on Outer Tab
9. Argon Glow Discharge Cleaning (Thin Film Tech.)
100 mTorr, 250 °C, 100 Å surface removal
10. Final Assembly and Cleaning at HTI

STEP 7: ELECTRODE/KOVAR PRE-CLEANING AT HTI

- a. Pre-determination/(pre-cleaning) of part contamination with SX-200, prior to introduction into CERN cleaning sequence.
- b. De-ionized water rinse at 60 °C for (specified) time.
- c. 300 °C bakeout (vacuum environment) for 2-4 hours with SX-200.
($10^{-5,6}$ Torr, small oven)
- d. 950 °C bakeout, without SX-200.
- e. Cool-down to ambient temperature per recommendations by Coors
(50 °F or 9 °F/min)
- f. Contaminant check at ambient temperature with SX-200.
- g. Wrap electrode/Kovar in double polyethelene bags, along with clear, explicit instructions to Coors to be handled with polyethelene gloves only: No direct contact with hands, and/or PVC (polyvinyl chloride) materials.
- h. Return to Coors in original packing box (if appropriate) for brazing.

Note: Electrode shall be supported vertically on ceramic edges with non-metallic materials (ceramics), thus avoiding any contact with metallized surfaces and possible mechanical distortion during oven bakeout.

STEP 10: FINAL ASSEMBLY AND CLEANING AT HTI

- a. Preparation and cleaning of all metal assemblies per Hutchinson procedure for CERN: cleaning in proprietary (phosphoric acid) liquid, 3 cascade rinses in de-ionized water, 950 °C bakeout of all metallic parts for (specified) time and (specified) cool-down.

Note: The critical transition temperature in steel at 750 °C must be traversed quickly to avoid material degradation.

- b. Weld frame to Kovar collar in inert atmosphere.
- c. 300 °C bakeout (vacuum environment) for 2-4 hours with SX-200.
- d. Test of electrode to Kovar vacuum seal with SX-200, and test of electrical resistivity of electrode to frame.
- e. Weld top and bottom plates, tubes, and valves.
- f. 300 °C bakeout (vacuum environment, with SX-200) for 2-4 hours to stress relieve weld.
- g. Reach 10^{-9} Torr at ambient temperature, close valve to SX-200.
- h. Helium leak test (vacuum environment in fixturing) with SX-200.
- i. De-ionized water rinse (17 M Ω cm) of vessel for (specified) time. Monitor input/output resistivity of de-ionized water.
- j. Verify cleanliness of Argon drying line with SX-200.

- k. Dry vessel with 100 °C pure Argon.
- l. Final test of electrical resistivity between electrode and frame.
- m. 300 °C bakeout (vacuum environment) for 48 hours with SX-200. Note: open filling ports of vessel should point to SX-200 analyzer head/ion pump ports for optimum molecular flow.
- n. Reach $\leq 10^{-9}$ Torr (with ion pump) at ambient temperature, confirming cleaning procedure; close valve to SX-200.
- o. Vent with pure Argon.
- p. Pack in double polyethelene sealed bags for shipment to Wiley Organics, Inc. All four (Nupro) valves shall be closed during shipment.

Note: Valves shall be LOCKED after filling at Wiley Organics, Inc.